Applied Energy 207 (2017) 176–194

Contents lists available at ScienceDirect

Applied Energy

journal homepage: www.elsevier.com/locate/apenergy

Corrective receding horizon scheduling of flexible distributed multi-energy microgrids

Ninoslav Holjevac [a,*], Tomislav Capuder [a], Ning Zhang [b], Igor Kuzle [a], Chongqing Kang [b]

[a] University of Zagreb Faculty of Electrical Engineering and Computing, Unska 3, 10000 Zagreb, Croatia
[b] Tsinghua University Department of Electrical Engineering, Haidian, Beijing, China

HIGHLIGHTS

- Defining optimal configuration between centralized and distributed MEM configurations.
- Flexibility of MEM increases with consideration of additional energy vectors.
- Annual operational costs are independent of the model approximations (e.g. MEM unit efficiency modelling).
- Significant errors occur if approximations are used for MEM daily operation analyses.

ARTICLE INFO

Article history:
Received 30 January 2017
Received in revised form 3 June 2017
Accepted 12 June 2017
Available online 24 June 2017

Keywords:
Multi-energy systems
Trigeneration
Flexibility
Uncertainty
Corrective scheduling

ABSTRACT

The goal of the paper is to provide a comprehensive operational flexibility evaluation of different Multi-energy Microgrid (MEM) options. This is done by incorporating Mixed Integer Liner Programming (MILP) model for annual simulations and expanding it with Receding Horizon Model Predictive Control (RH-MPC) algorithm for short term daily operational analyses. The model optimizes flows of various energy vectors: heat, fossil fuels (natural gas), cooling and electricity, coordinating different microgrid elements with the goal of serving final consumer needs and actively participating in energy markets.

The second novelty of the work is in the approach to multi-energy operational flexibility assessment, capturing different technologies, MEM configurations and different modelling concepts. When MEM is connected to the upstream power system its flexibility manifests as capability to alleviate variability and uncertainty in local production of RES and demand. On the other hand, when operating isolated from the rest of the system, the main flexibility indicator is minimum waste of energy while ensuring the satisfaction of all demand needs (electrical and heating/cooling). Following on this, multiple MEM configurations have been analyzed, showing different levels of available flexibility and capability to follow scheduled day-ahead exchange with the rest of the system, but also different amounts of wasted/curtailed energy in off-grid mode. Additionally, detailed analyses are performed concerning algorithm approximations which are often introduced in MEM modelling, such as efficiency of generation units. While these approximations have smaller impact on annual operational flexibility assessment (the difference is around 2–5% in terms of total cost), the result clearly show their significant impact on daily operational flexibility estimates.

1. Introduction

1.1. Introduction and motivation

Integration of renewable energy sources today is largely driven by incentives [1] and general goal of the European Union to increase the share of zero emission generation [2]. However, passive integration of these sources close to the consumers might result in significant over investments driven by needed improvements on the distribution grid level [3,4]. In addition, the idea and design of all renewable energy system (RES) [5] and global energy policy [6] should be put hand in hand with the latest strategic goal announced in Europe; at least 50% of energy production should be in the hands of final consumers [7]. This also means that a significant share of operational flexibility, alleviating above mentioned issues, will come from the distribution level through integration of technologies capable of responding to different price

* Corresponding author.
E-mail addresses: ninoslav.holjevac@fer.hr (N. Holjevac), tomislav.capuder@fer.hr (T. Capuder), ningzhang@tsinghua.edu.cn (N. Zhang), igor.kuzle@fer.hr (I. Kuzle), cqkang@tsinghua.edu.cn (C. Kang).

http://dx.doi.org/10.1016/j.apenergy.2017.06.045
0306-2619/

signal. Evaluating the potential flexibility benefits of different technologies in the distribution level microgrids provides a valuable step towards a successful integration of renewable energy sources that will complement the low carbon technologies on a larger scale [8].

Microgrid is defined as a set of consumers, distributed generation and energy storages coordinated with the aim of achieving reliable supply for final consumers and exchanging predefined energy with the rest of distribution system through a point of common coupling (PCC) [9]. Scheduling microgrid operation is subject to imperfect forecasting of local RES or demand, however if these imbalances are compensated on the local level microgrids become flexible nodes capable of providing multiple flexibility services to the upstream system thus enabling larger integration of RES [10,11] (Fig. 1). Aggregating consumers of different energy vectors (electricity, gas, cooling) and distributed multi-generation sources on the same location with coupled centralized control is the main advantage of a multi-energy microgrid (MEM) concept.

Power system flexibility is becoming a key characteristic in answering the increasing share of variable generation. Technically, it can be defined as the ability to respond to changes in demand/generation equilibrium [12]. In economic sense, the flexibility can be defined as the capability of a single market subject to quickly adjust to most current market situation and follow the scheduled plan of exchange [13]. All power systems inherently have a certain flexibility level; with increase of unpredictable and variability RES these values are much higher. Lack of system flexibility can be manifested in frequency deviations which can lead to load shedding, deviations from contracted exchanges, wind curtailment, higher price volatility. The current system flexibility requirements are mostly based on deterministic calculation which increases the system costs and does not include variables that stretch through several time periods (intertemporal constraints) [14].

Traditionally all the imbalance between the production and consumption had to be compensated by centralized unit, however with the advent of new technologies (μCHP, electric vehicles, flexible demand, electric heat pumps etc.) new flexibility potential can be unlocked on the local, distribution level [15–17]. Concepts of a virtual power plants and microgrids (e.g. [18,19]) are well known, yet there is still a lack of integral approach to all energy vector assessment on a microgrid level, particularly in terms of interaction between the MEM and the rest of the system. This paper tackles the operational aspects also providing some valuable inputs for planning, optimal sizing of microgrid elements [20] and business cases [21].

1.2. Current research

While integration of batteries and electric vehicles is widely researched for their capability to provide these flexibility services [22], it is equally important, if not more, to unlock the already existing flexibility in the distribution level energy systems. In this context multi-energy systems (MES) [23] and multi-energy microgrids (MEM) become increasingly relevant by coupling different units and shifting between energy vectors. Such systems have the capability of providing required services for the consumer without diminishing the comfort of final users and, on the other hand, to provide response to system requirements on different and multiple time frames [24,25]. Several research papers have shown significant benefits by means of adaptive dispatch and coordination of multi-energy systems in active distribution networks [26].

In order to utilize provision of price driven services from multi-energy entities such as MEM, or other flexible units at the distribution side, they need to be aggregated into a single entity since such market participation increases both market visibility, capability to compete in multiple market and, correspondingly, their benefits [27]. Aggregation in the concept of virtual power plants (VPP) is usually composed of conventional and renewable energy units (RES) [28,29]. The inability to forecast RES generation of the VPP defines participation of such units in the market, where flexible units such as storage are put in service of minimizing the level of variability and uncertainty announced ahead of realization of production [30,31]. Recent research focuses on robust or risk-based bidding strategies to overcome these issues [32], however such approach can lead to conservative solutions and non-optimal operating points. It is interesting to notice that already single MEM unit can be regarded as VPPs, since they are usually composed of several units coupled together [33]. Cooperation of these units results in both economic savings and environment impact reduction compared to separate production [34]. When grouping different multi-energy units the value of multiple energy vector shifting becomes even more highlighted [35].

On a microgrid level the local heat and cooling demands are more or less predictable and do not contribute significantly to uncertainty and variability; unlike local RES production. In addition, heat and cooling have a significant amount of inertia

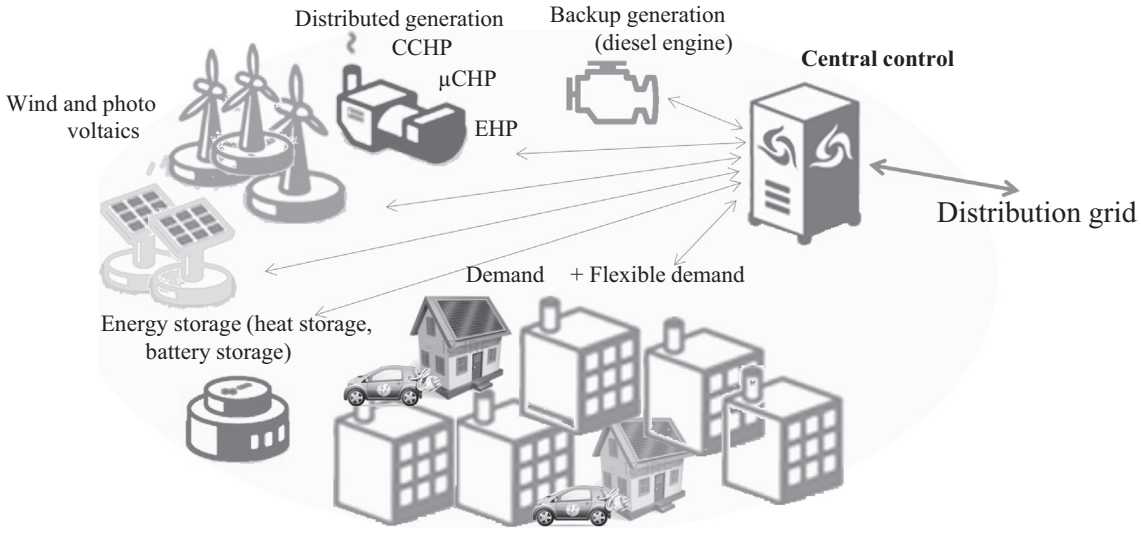

Fig. 1. Microgrid elements and the potential of connection of a multi-energy microgrid as a flexible multi-energy node through a PCC.

meaning that their moment-to-moment load balancing requests are less strict. Previous work of authors [36] demonstrates an adaptive receding horizon for re-dispatching MES units with the goal of minimizing deviations from the announced schedule as well as maximizing the usage of electricity locally generated from RES. However, it does not fully capture MES capability as it only analyses a specific microgrid environment and does not focus on estimating flexibility potential outside optimal energy provision. The value of re-dispatching capability is also recognized through the concept of MES profitability maps [37], however with no optimization through a receding horizon.

1.3. Contributions

This paper provides relevant contributions in quantifying flexibility capacities of multi-energy microgrid. For this purpose, an adaptive receding MILP optimization model is developed. The analyses focus on defining the impact of:

(a) Different compositions of MEM. In particular, the benefits of decentralized MEM units compared to a single central energy community unit. All analyzed options provide electricity, heat and cooling to the final consumer, without diminishing their comfort, through different trigeneration unit technologies and belonging efficiencies.

(b) Modelling aspects and approximations. The paper clearly demonstrated how common modelling approximations can be negligible in annual simulations (performed for planning purposes) but result in rather different short term operation states (analyses for day ahead scheduling). These approximations are of critical importance in assessing operational flexibility as they might lead to incorrect results and conclusions.

(c) Both of the above aspects are evaluated through several defined MEM flexibility indicators, wasted heat and curtailed wind, considering operational techno-economic constraints of different microgrid components (battery storage, heat storage, micro combined heat and power units (μCHP) in off-grid (islanded) mode and interaction with the distribution system through the point of common coupling (PCC) in on-grid (parallel) mode.

The work presented here is a substantial extension of material presented by the authors in [38], however for easier understanding some of the model segments will be repeated and elaborated in the following sections.

2. Nomenclature and abbreviations

Input parameters in order of appearance		
τ	Simulation time step duration (number of hour segments ΔT of an hour)	Section 3.0
T	Simulation duration [h]	Section 3.0
t	Current simulation step	Section 3.0
i	Counter referring to *i-th* ho usehold	Section 3.0
K	Total number of households	Section 3.0
η^{cchp_e}	Electricity production efficiency of the district CCHP unit [%]	Section 3.1
η^{cchp_h}	Heat production efficiency of the district CCHP unit [%]	Section 3.1
$H^{CCHP}_{\max}$, $H^{CCHP}_{\min}$	Maximum/minimum output of the district CCHP unit [kW h]	Section 3.1
$ramp$	Ramping characteristic of the district CCHP unit [kW h/ΔT]	Section 3.1
$H^{CHP}_{\max,i}$, $H^{CHP}_{\min,i}$	Maximum/minimum heat output of a household μCHP unit [kW h]	Section 3.2
$\eta^{chp\_e}_i$	Electricity production efficiency of household μCHP unit [%]	Section 3.2
$\eta^{chp\_h}_i$	Thermal energy production efficiency of household μCHP unit [%]	Section 3.2
$H^{EHP}_{\max,i}$	Household EHP unit maximum thermal output [kW h]	Section 3.3
$COP_{t,i}$	Household EHP coefficient of performance	Section 3.3
$H^{ab}_{\max,i}$	Household auxiliary boiler unit maximum heating output [kW h]	Section 3.4
η^{AB}	Household auxiliary boiler unit efficiency [%]	Section 3.4
$C^{hs}_{\max,i}$	Household heat storage maximum capacity [kW h]	Section 3.4
λ^{hs}_i	Household heat storage unit hourly losses [%]	Section 3.4
$C^{TES}_{\max}$, $C^{TES}_{\min}$	District thermal energy storage maximum/minimum capacity [kW h]	Section 3.5
λ^{TES}	District thermal energy storage unit hourly losses [%]	Section 3.5
$C^{BAT}_{\max}$, $C^{BAT}_{\min}$	Central battery storage maximum/minimum capacity [kW h]	Section 3.6
η^{ch}_{BAT}, η^{dch}_{BAT}	Battery storage charge/discharge efficiency [%]	Section 3.6
$C^{BAT\_dist}_{\max,i}$, $C^{BAT\_dist}_{\min,i}$	Household battery unit maximum/minimum capacity [kW h]	Section 3.6
λ^{BAT}	Central battery storage self-discharge rate [%]	Section 3.6
λ^{BAT_dist}	Distributed battery self-discharge rate [%]	Section 3.6
$Cool^{ABC}_{\max}$	Absorption chiller maximum cooling output [kW h]	Section 3.7
COP^{ABC}	Coefficient of performance of absorption chiller	Section 3.7
$Cool^{EC}_{\max}$	Electric (compression) chiller maximum cooling output [kW h]	Section 3.7

(*continued*)

Input parameters in order of appearance		
COP^{EC}	Coefficient of performance of electric (compression) chiller	Section 3.7
$Cool^{AC}_{\max,i}$	Household AC unit maximum cooling output [kW h]	Section 3.7
COP^{AC}	Coefficient of performance of household air-condition (AC) unit	Section 3.7
$E^{DIESEL}_{\max}$	Backup diesel generator maximum electricity output [kW h]	Section 3.8
η^{DIESEL}	Backup diesel generator efficiency [%]	Section 3.8
$C^{flex}_{\max}$	Maximum capacity of flexible demand being rescheduled [%]	Section 3.9
p^{flex}	Percentage of total electrical demand regarded as flexible demand [%]	Section 3.9.
E^{wind}_t	Average hourly wind production of 1 kW installed capacity [kW h]	Section 3.9
E^{PV}_t	Average hourly PV production of 1 kW installed capacity [kW h]	Section 3.9
$H^{d}_{t,i}$	Household heat demand [kW h_t]	Section 3.10
$E^{d}_{t,i}$	Household electricity demand [kW h_e]	Section 3.10
$Cool^{d}_{t,i}$	Household cold demand [kW h_e]	Section 3.10
EM_t	Average emissions for electricity production [g/kW h]	Section 3.11
EM^{ng}	Natural gas average emission[g/kW h]	Section 3.11
c^{ng}	Natural gas supply price [€/kW h]	Section 4.0
c^{diesel}	Diesel supply price [€/kW h]	Section 4.0
c^{fuel}	District CCHP unit fuel supply price [€/kW h]	Section 4.0
$c^{imp}_t, c^{\exp}_t$	Electricity price [€/kW h]	Section 4.0
M^{sell}, M^{buy}	Imbalance price modification factors	Section 4.0
P^{heat}, P^{wind}	Inhibiting factor for waste of heat and curtailment of wind	Section 4.0
Decision variables in order of appearance		
H^{CCHP}_t	Heat output of the district CCHP unit [kW h]	Section 3.1
E^{CCHP}_t	Electricity output of the district CCHP unit [kW h]	Section 3.1
$H^{binCCHP}_t$	Binary variable for the operational state of the CCHP unit	Section 3.1
$H^{startupCCHP}_t$	Binary variable for the startup signal of the CCHP unit	Section 3.1
F^{CCHP}_t	Fuel intake consumption of the district CCHP unit [kW h]	Section 3.1
$H^{CHP}_{t,i}$	Heat output of the household μCHP unit [kW h]	Section 3.2
$H^{binCHP}_{t,i}$	Binary variable for the operational state of the household μCHP unit	Section 3.2
$E^{CHP}_{t,i}$	Electricity output of the household μCHP unit [kW h]	Section 3.2
$F^{CHP}_{t,i}$	Fuel intake consumption of the household μCHP unit [kW h]	Section 3.2
$H^{EHP}_{t,i}$	Household EHP unit thermal power output [kW h]	Section 3.3
$E^{EHP}_{t,i}$	Household EHP unit electrical power output [kW h]	Section 3.3
$H^{binEHP}_{t,i}$	Household EHP unit thermal power binary variable	Section 3.3
$Cool^{EHP}_{t,i}$	Household EHP unit cooling power output [kW h]	Section 3.3
$Cool^{binEHP}_{t,i}$	Household EHP unit cooling power binary variable	Section 3.3
$H^{AB}_{t,i}$	Household auxiliary boiler unit heat production [kW h]	Section 3.4
$fuel^{AB\_total}_t$	Household auxiliary boiler units total fuel usage [kW h]	Section 3.4
$H^{hs}_{t,i}$	Household heat storage net heat flow[kW h]	Section 3.4
$C^{hs}_{t,i}$	Household heat storage capacity at simulation step t [kW h]	Section 3.4
C^{TES}_t	District thermal energy storage capacity at simulation step t [kW h]	Section 3.5
$H^{CCHP\_TES}_t$	Heat flow to district TES from CCHP unit [kW h]	Section 3.5
H^{TES}_t	Heat flow from TES to consumers [kW h]	Section 3.5
$E^{BAT\_ch}_t$	Central battery storage charging power [kW h]	Section 3.6
$E^{binBAT\_ch}_t$	Central battery storage charging power binary variable	Section 3.6
$E^{BAT\_dch}_t$	Central battery storage discharging power [kW h]	Section 3.6
$E^{binBAT\_dch}_t$	Central battery storage discharging power binary variable	Section 3.6
C^{BAT}_t	Central battery storage capacity [kW h]	Section 3.6

(*continued on next page*)

(*continued*)

Input parameters in order of appearance		
$E_{t,i}^{BAT\_ch}$	Household battery unit charging power [kW h]	Section 3.6
$E_{t,i}^{binBAT\_ch}$	Household battery unit charging power binary variable	Section 3.6
$E_{t,i}^{BAT\_dch}$	Household battery unit discharging power [kW h]	Section 3.6
$E_{t,i}^{binBAT\_dch}$	Household battery unit discharge power binary variable	Section 3.6
$C_{t,i}^{BAT\_dist}$	Household battery unit capacity [kW h]	Section 3.6
$Cool_t^{ABC}$	Absorption chiller cooling output [kW h]	Section 3.7
$Cool_t^{EC}$	Electric (compression) chiller cooling output [kW h]	Section 3.7
$Cool_{t,i}^{AC}$	Household AC unit cooling output [kW h]	Section 3.7
E_t^{DIESEL}	Backup diesel generator electricity output [kW h]	Section 3.8
$E_t^{binDIESEL}$	Backup diesel generator operational binary variable [kW h]	Section 3.8
$E_t^{startupDIESEL}$	Backup diesel generator startup binary variable [kW h]	Section 3.8
E_t^{flex}	Flexible demand being rescheduled [kW h]	Section 3.9
$E_t^{wind\_real}$	Produced energy from wind [kW h]	Section 3.9
$E_t^{wind\_curt}$	Curtailed wind energy [kW h]	Section 3.9
X^{wind}	Installed wind power capacity [kW]	Section 3.9
X^{PV}	Installed PV capacity [kW]	Section 3.9
F_t^{ng}	Total natural gas energy consumed [kW h]	Section 3.11
F_t^{DIESEL}	Total diesel fuel energy consumed [kW h]	Section 3.11
$long_t^{imp}$	Positive mismatch in import compared to day-ahead contracted exchange [kW h]	Section 4.0
$long_t^{\exp}$	Positive mismatch in export compared to day-ahead contracted exchange [kW h]	Section 4.0
$short_t^{imp}$	Negative mismatch in import compared to day-ahead contracted exchange [kW h]	Section 4.0
$short_t^{\exp}$	Negative mismatch in export compared to day-ahead contracted exchange [kW h]	Section 4.0
Abbreviations		
RES	Renewable Energy Sources	Section 1.1
MEM	Multi-energy Microgrid	Section 1.1
μCHP	Micro Combined Heat and Power	Section 1.3
MILP	Mixed Integer Linear Programming	Section 1.3
COP	Coefficient of Performance	Section 3.0
CCHP	Combined Cooling, Heat and Power (trigeneration)	Section 3.0
EHP	Electric Heat Pump	Section 3.0
PV	Photovoltaic	Section 3.0
AB	Auxiliary Boiler	Section 3.4
TES	Thermal Energy Storage	Section 3.5
RH-MPC	Receding Horizon Model Predictive Control	Section 4.0

3. Multi-energy microgrid modelling

The model of multi-energy microgrid includes all relevant components to analyze the interactions between the elements and energy vectors. The developed model in this paper, as mentioned before, presents a substantial expansion of the work done in [38]. The residential community model can consists of any number of households and each household can be equipped with different energy sources and has various demand curves (heating, cooling and electricity). Depending on the microgrid configuration each household is supplied by either district CCHP or household μCHP unit, district ground source EHP or household air-water EHP unit (cooling and heating) with addition of household auxiliary boilers, household heat storages, battery storages and household installed RES units (PV panels). Additionally, the model considers flexible demand response and operation of a central battery storage. The model is easily expendable and new additional elements (e.g. electric vehicles) can be added. For the test-case analysis purposes size of the microgrid community has been chosen to consist of 300 households. The model relies on the following assumptions:

(a) Sampling time is constant (simulation time step τ which enables a clear connection between power and produced energy and that way the model is able to capture different time step resolutions);
(b) Flexible consumers' response in rescheduling their demand is not compensated and that financial aspect is not accounted for;
(c) Developed MEM model assumes the microgrid is not big enough to be considered as price-maker;
(d) MEM operation is considered just from market perspective where voltage and frequency stability issues are not regarded;
(e) No communications error or delay was considered for the central controller, which is assumed to have all needed data available;

The schematic diagram of modelled MEM is shown in Fig. 2 for scenario where all elements are installed on a household level. The blue arrow represents the flow of electrical energy. Yellow arrow represents the heat energy flow. Green arrow represents flow of

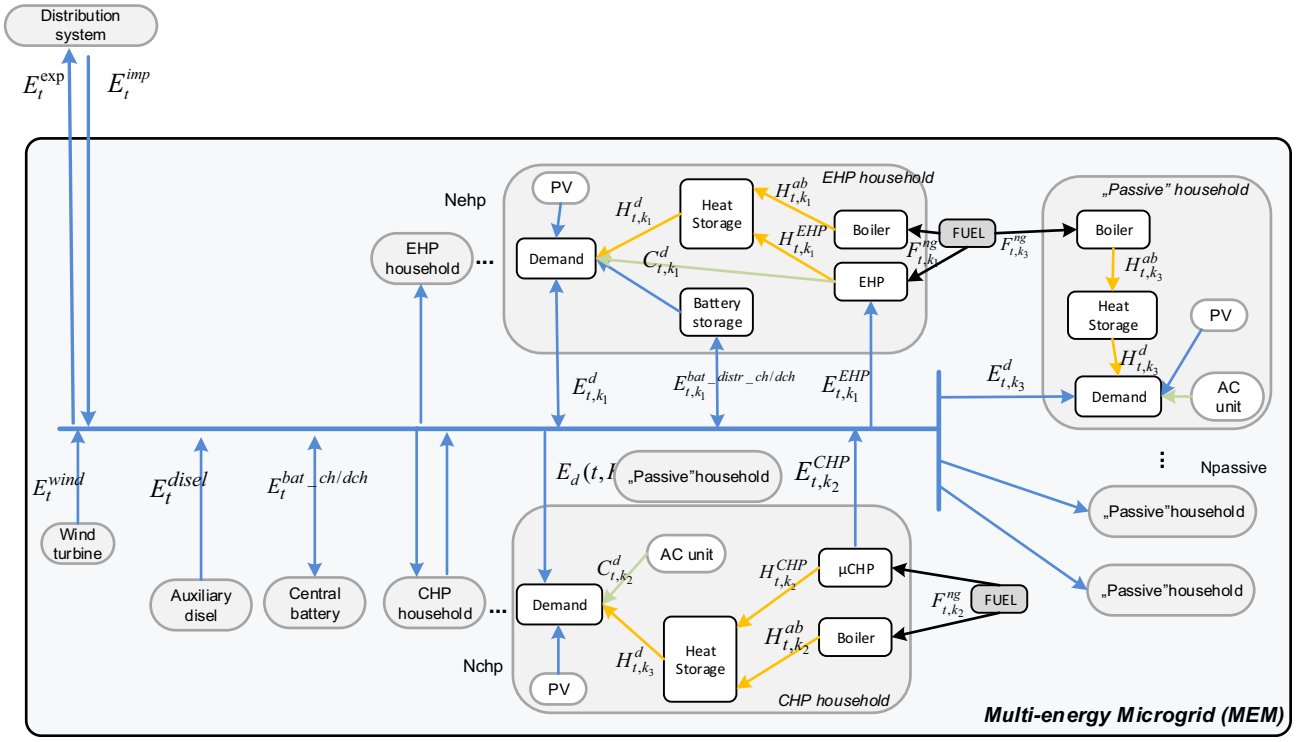

Fig. 2. MEM model schematic for proposed distributed household configuration.

cooling energy. Red arrow shows natural gas flows, and central bus in the first case represents electrical network. The flexibility potential is unlocked through the electrical grid when the operation of, for example, µCHP and EHP is coupled.

The concept of installing larger, central district units is shown in Fig. 3. The central bus represents the district heating/cooling network and electrical network. Different combinations of district and household elements are also possible.

Multi-energy microgrid elements can be installed on the household level in distributed manner (smaller units) or they can be centralized on the district level (larger units) as mentioned before. For the purpose of this paper, the following MEM configuration are selected and shown in Table 1.

Type 1 assumes all elements are installed on the household level: local EHP (Electric Heat Pumps) and µCHP (micro Combined Heat and Power units). Type 2 assumes centralized heat and elec-

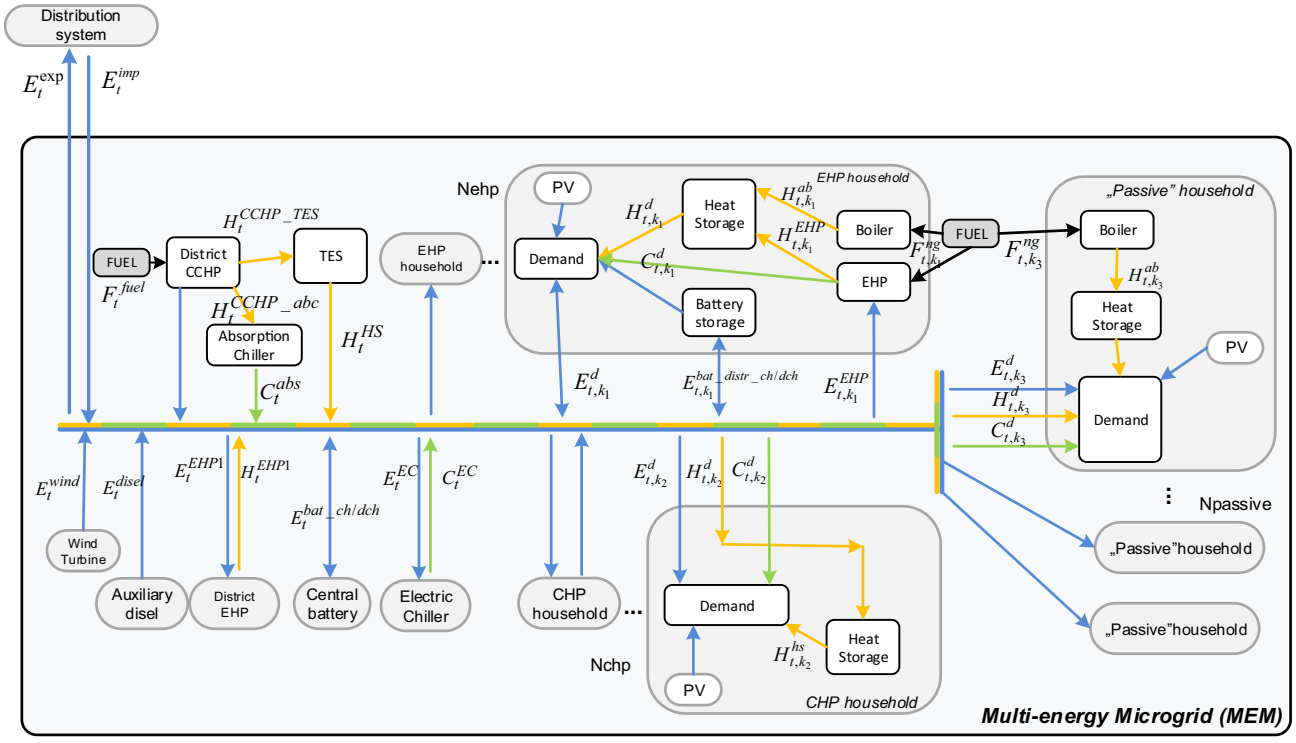

Fig. 3. MEM model schematic for proposed centralized district configuration.

Table 1
Proposed different structures of multi-energy microgrid.

Microgrid configuration suggestion	CHP		EHP		Thermal storage		Battery storage		Chillers	Backup diesel	RES	
	District	House.	District	House	District	House.	District	House.			PV	Wind
Type 1 – distributed	–	✓	–	✓	–	✓	–	✓	–	–	✓	✓
Type 2 – centralized	✓	–	✓	–	✓	–	✓	–	✓	✓	✓	✓
Type 3 – CCHP+ household EHP	✓	–	–	✓	✓	✓	✓	–	✓	–	✓	✓
Type 4 – district EHP+ μCHP	–	✓	✓	–	–	✓	–	✓	–	✓	✓	✓

tricity production in a district CCHP unit. Type 3 assumes that a certain share of households is supplied by centralized CCHP (Combined Cooling Heat and Power) and this share is equal to households supplied by μCHP and boiler in Type 1 while the remainder of households still use local EHP as a primary energy source. Type 4 assumes part of households uses district EHP while the remainder keeps μCHP and boiler as electricity/heating source.

Efficiencies of selected production units' efficiencies have significant impact MEM operation. These units, such as μCHP, CCHP and EHP units are modelled in two ways:

(1) Typical efficiency approximations modelling approach, presented as a single constant value (COP for EHP, thermal and electrical efficiency for μCHP/CCHP unit).
(2) Varying efficiency (varying COP, efficiency curves for μCHP/CCHP depending on loading).

More detailed models increase the computational times and in some cases they are not justified [39,40] but even a slight increase in accuracy results in significant differences, as it will be shown in the results section.

3.1. Combined cooling, heat and power (CCHP) units

For the district CCHP units, different installed capacities can be considered. The production of heat and power is coupled. The productions of heat and power are defined at each time step starting from the fuel input F_t^{CHP1} through relevant thermal efficiency η_{chp_h1} and electrical efficiency η_{chp_e1}. For μCHP and smaller CCHP units electrical and thermal efficiencies, as mentioned before, are typically a function of the loading curve. This aspect is often, for the sake of simplicity, not regarded and the approximation stating that efficiencies are constant is commonly made [41–43].

$$E_t^{CCHP} = F_t^{CCHP} \cdot \eta^{cchp\_e} \tag{1}$$

$$H_t^{CCHP} = F_t^{CCHP} \cdot \eta^{cchp\_h} \tag{2}$$

This means the connection between production of heat and electricity can be expressed as shown by Eq. (3) if constant efficiencies are considered:

$$E_t^{CCHP} = \frac{H_t^{CCHP} \cdot \eta^{cchp\_e}}{\eta^{cchp\_h}} \tag{3}$$

The CCHP thermal output is limited by the uppers limit $H_{\max}^{CCHP}$ which represents its maximum output power, and its lower operating limit $H_{\min}^{CCHP}$ which can be considered as minimum stable generation point (MSG). The binary variable $H_t^{binCCHP}$ indicates the unit is operational if its value is 1, and that unit is off if the value is 0. The CCHP production is bounded by its upper and lower limit expressed as:

$$H_t^{binCCHP} \cdot H_{\min}^{CCHP}/\tau \leqslant H_t^{CCHP} \leqslant H_t^{binCCHP} \cdot H_{\max}^{CCHP}/\tau \tag{4}$$

Startup binary logic is expressed as shown by Eq. (5).

$$H_t^{startupCCHP} = H_t^{binCCHP} - H_{t-1}^{binCCHP} \tag{5}$$

For smaller units considered in this paper (power output in range of e.g. 1000 kW) the minimum up time and minimum off time can be neglected and is not considered.

Since thermal power plants like considered district CCHP unit typically exhibit variations in power output, ramping constraints that limit the output increase or decrease between two successive time periods is added (Eq. (6)). Constraint *ramp* is expressed in comparison to maximum output power as $H_{\max}^{CCHP}/\tau$.

$$-ramp \leqslant H_t^{CCHP} - H_{t-1}^{CCHP} \leqslant ramp \tag{6}$$

If more detailed model is considered regarding the efficiency of operation the mathematical model for this mode 2 of operation is extended and therefore Eqs. (2) and (3) that model the output power are substituted by the following formulations (Eqs. (7) and (8)) that have an aim to capture the non-linear behavior of the efficiencies.

$$E_t^{CCHP} = F_t^{CCHP} \cdot \eta^{cchp\_e} + H_t^{binCCHP} \cdot \eta^{cchp\_e'} \tag{7}$$

$$H_t^{CCHP} = F_t^{CCHP} \cdot \eta^{cchp\_h} + H_t^{binCCHP} \cdot \eta^{cchp\_h'} \tag{8}$$

The efficiencies are modelled as linear approximations while full-load efficiency is considered to be the same for both modes of operation. The coefficient $\eta_{chp\_e1}, \eta_{chp\_e1'}$ and $\eta_{chp\_h1}, \eta_{chp\_h1'}$ for units of different sizes have different values in order to preserve the same efficiency curve shape with respect to part-load operation conditions. For example, the unit of maximum power (fuel intake maximum limit) of 2000 kW the coefficient values are $\eta^{cchp\_e} = 0.37, \eta^{chcp\_e'} = -107,42$ and $\eta^{cchp\_h} = 0.65, \eta^{cchp\_h'} = -197,10$. For 1000 kW the values are $\eta^{cchp\_e} = 0.42, \eta^{cchp\_e'} = -90,43$ and $\eta^{cchp\_h} = 0.70, \eta^{cchp\_h'} = -147,90$, describing the efficiency of Capstone units [44].

The CCHP units usually have two operating modes, namely electricity following and heat/cooling demand following [45]. This paper assumes heat/cooling following mode of operation.

3.2. Micro Combined heat and power (μCHP) units

Distributed μCHP units are installed in a number of households, depending on the scenario. In Eq. (9) the coefficient τ is a time step and used as a direct connection between power and energy. The μCHP units considered in this work have installed capacity of 8 kW_t and technical minimum of 1.6 kW_t.

$$H_{t,i}^{binCHP} \cdot H_{\min,i}^{CHP} \cdot \tau \leqslant H_{t,i}^{CHP} \leqslant H_{t,i}^{binCHP} \cdot H_{\max,i}^{CHP} \cdot \tau \tag{9}$$

It is assumed these micro units can adjust their power fast enough and therefore no ramping constraints have been added. As a reference Capstone units C30 and C200 were used [46–48]. The tests have shown that these units are characterized by under 120 s response in start, stop and power adjustments, while the shutdown process is over in 200 s. This also means that for the time frame considered in this paper, these constraints can be neglected [49].

Again μCHP units are modelled in two ways with respect to the efficiency. The first is the constant efficiency according to which the output of *i-th* μCHP is:

$$E_{t,i}^{CHP1} = \frac{H_{t,i}^{CHP1} \cdot \eta_i^{chp\_e}}{\eta_i^{chp\_h}} \tag{10}$$

Total fuel (natural gas) consumption of all μCHP in heat following mode is:

$$fuel_t^{CHP\_total} = \sum_i^K \frac{H_{t,i}^{CHP}}{\eta_i^{chp\_h}} \tag{11}$$

The second mode assumes variable efficiency depending on the loading conditions.

$$E_{t,i}^{CHP} = F_{t,i}^{CHP} \cdot \eta_i^{chp\_e} + H_{t,i}^{binCHP} \cdot \eta_i^{chp\_e'} \tag{12}$$

$$H_{t,i}^{CHP} = F_{t,i}^{CHP} \cdot \eta_i^{chp\_h} + H_{t,i}^{binCHP} \cdot \eta_i^{chp\_h'} \tag{13}$$

The coefficient values for electrical output are $\eta_i^{chp\_e} = 0.55$, $\eta_i^{chp\_e'} = 4.51$ making the approximations close to the Capstone commercial unit (Fig. 4).

3.3. Electric heat pump (EHP) units

Similar to CHP, both local and district EHP units are considered as energy providers. In the model a number of households use heat generated by EHP as a main heat and cooling source. Eq. (14) describes the relation between the current heat output and electricity consumption for a household unit and Eq. (14) describes the relation for larger EHP unit.

$$H_{t,i}^{EHP} = E_{t,i}^{EHP} \cdot COP_t \tag{14}$$

$$H_t^{EHP} = E_t^{EHP} \cdot COP_t \tag{15}$$

EHP heat and cooling productions are limited by their upper and lower boundaries [43]. The electric heat pump can operate in either cooling or heating mode while the maximum output power is assumed to be similar [50] and modelled by Eq. (18).

$$0 \leqslant H_{t,i}^{EHP} \leqslant H_{\max,i}^{EHP} \cdot \tau \cdot H_{t,i}^{EHPbin} \tag{16}$$

$$0 \leqslant Cool_{t,i}^{EHP} \leqslant Cool_{\max,i}^{EHP} \cdot \tau \cdot Cool_{t,i}^{EHPbin} \tag{17}$$

$$H_{t,i}^{EHPbin} + C_{t,i}^{EHPbin} \leqslant 1 \tag{18}$$

For household units air-water type of electric heat pump is assumed. Its efficiency ratio depends on the outdoor temperature and temperature difference between outside air and heated space. Diplex and Acadia heat pumps were used as a reference [50,51]. The assumed type of central EHP is ground source. The COP also depends on loading conditions [52] but the effect of temperature difference is much more significant [53,54].

Ground source heat pumps demonstrate higher COP compared to smaller air-water heat pumps and their COP is less variable between seasons and throughout the day.

3.4. Household auxiliary boiler (AB) units and household heat storage (HS) units

Households that have no other active heat source are equipped with boiler units as primary source of heat while houses with μCHP and EHP have boilers as a backup option. The boilers are fueled by natural gas and peak heat output power is 10 kW_t with efficiency of fuel conversion 81%. The gas boiler could be substituted with the electricity boiler that consumes electric power to generate heat when load cannot be satisfied by CHP units for example. The efficiency of larger boiler units can also be modelled as constant or variable [55,56], but the assumption in this paper was that the smaller household boiler units operate with constant efficiency.

$$H_{t,i}^{AB} \leqslant H_{\max,i}^{AB} \cdot \tau \tag{19}$$

$$fuel_t^{AB\_total} = \sum_i^K \frac{H_{t,i}^{AB}}{\eta^{AB}} \tag{20}$$

Furthermore, to increase the reliability of heat supply and overall flexibility, all household are equipped with a heat storage tank in form of a simple water tank. Assumed maximum storage capacity $C_{\max,i}^{hs}$ is 6 kW h which translates into approximately 0.15 m^3 water tank [57]. Total thermal energy available in the storage in each time step is expressed as thermal energy stored the previous time step plus the net heat thermal storage flow (Eq. (21)). The hourly loses λ_i^{hs} are assumed to be 4%.

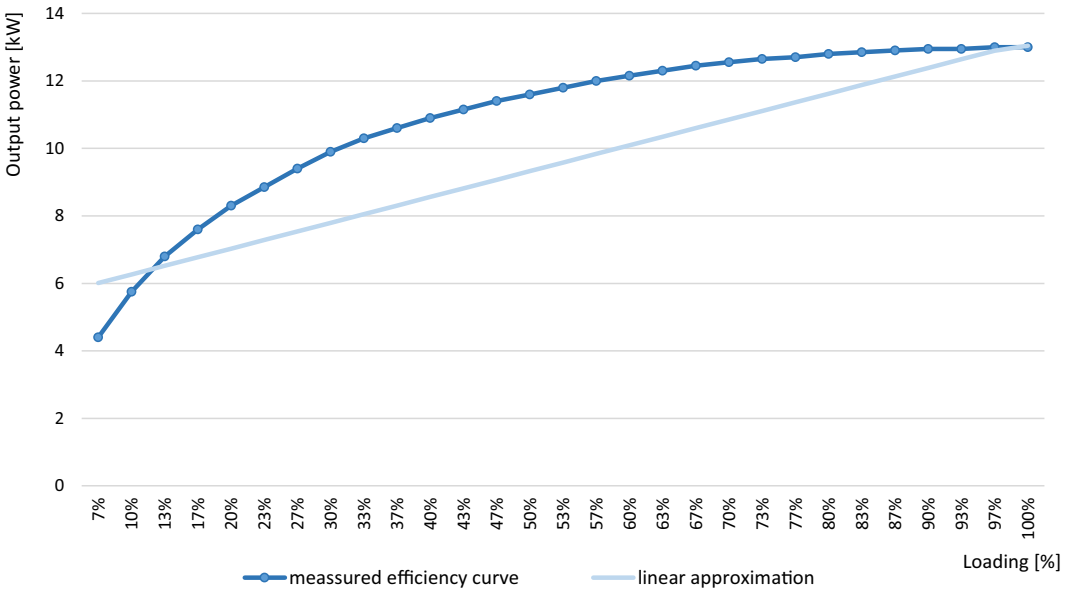

Fig. 4. μCHP unit variable efficiency linear approximation.

$$C_{t,i}^{hs} = (1 - \lambda_i^{hs}/\tau) \cdot C_{t-1,i}^{hs} - H_{t,i}^{hs} \quad (21)$$

The maximum heat storage capacity is limited (Eq. (22)) as well the charge/discharge time (Eq. (23))

$$C_{t,i}^{hs} \leqslant C_{\max,i}^{hs} \quad (22)$$

$$H_{t,i}^{hs} = C_{\max,i}^{hs} \cdot \tau \quad (23)$$

3.5. Central thermal energy storage (TES) unit

As stated before the electricity and heat energy generated by the CCHP units are coupled. In order to increase the flexibility of this district system, thermal energy storage is added. Similar sizing and modelling approach is taken as in [58]. The thermodynamic process of the heat flow in the heat storage is a complex process. More detailed models (e.g. stratified model) increase the complexity and computational burden, however simple models, that assume ideally mixed volume with homogeneous temperature, provide results that are precise enough [39]. The model used in this paper is described by the Eqs. (24), (25) and (26) which consider the intertemporal variable of storage capacity, charge/discharge and maximum capacity limit. The model is similar to commonly used models (e.g. [59]).

The charging flow is heat energy supplied by the CCHP unit and discharging flow is the heat supplied to the consumers.

$$C_t^{TES} = (1 - \lambda^{TES}/\tau) \cdot C_{t-1,i}^{hs} - H_t^{TES} + H_t^{CCHP\_TES} \quad (24)$$

$$C_{\min}^{TES} \cdot 2\tau \leqslant H_t^{TES} \leqslant C_{\max}^{TES} \cdot 2\tau C_{\min}^{TES} \cdot 2\tau \leqslant H_t^{CCHP\_TES} \leqslant C_{\max}^{TES} \cdot 2\tau \quad (25)$$

$$C_{\min}^{TES} \cdot \tau \leqslant C_t^{TES} \leqslant C_{\max}^{TES} \cdot \tau \quad (26)$$

Hourly losses λ_i^{TES} are assumed to be 0.1% (total water volume ≈200 m^3) and 80% is assumed for a cycle efficiency. Initial thermal energy storage capacity is assumed to be $C_{\max}^{TES}/4$.

3.6. Battery storage

3.6.1. Central battery storage

The battery for a central model is incorporated with the following equations (Eqs. (27)–(30)). Maximum value of energy flow through battery (charge/discharge) at any given time step is limited and connected with the maximum capacity of the battery (Eq. (27)). It is assumed that, for example, in a time simulation step of a half an hour the battery can be charged to one eight of its capacity. The binary logic that ensures both charge and discharge cannot occur at the same time is expressed as Eq. (29). Battery capacity is limited with its maximum capacity and minimum capacity to prevent deep discharging (Eq. (30)).

$$0 \leqslant E_t^{BAT\_ch} \leqslant C_{\max}^{BAT}/(\tau \cdot 4) \cdot E_t^{binBAT\_ch} \quad (27)$$

$$0 \leqslant E_t^{BAT\_dch} \leqslant C_{\max}^{BAT}/(\tau \cdot 4) \cdot E_t^{binBAT\_dch} \quad (28)$$

$$E_t^{binBAT\_dch} + E_t^{binBAT\_chh} \leqslant 1 \quad (29)$$

$$C_{\min}^{BAT} \leqslant C_t^{BAT} \leqslant C_{\max}^{TES} \quad (30)$$

The capacity of central battery between two successive time steps changes according to Eq. (31). Self-discharging loss (λ^{BAT}) is regarded as the loss of 0.005% of stored energy per hour.

$$C_t^{BAT} = (1 - \lambda^{BAT} \cdot \tau) \cdot C_{t-1}^{BAT} + E_t^{BAT\_ch} \cdot \eta_{BAT}^{ch} + E_t^{BAT\_dch}/\eta_{BAT}^{dch} \quad (31)$$

3.6.2. Household battery storage

On the other hand, the battery model for the batteries distributed among households (K is the number of households) is described with the following constraints:

$$0 \leqslant E_{t,i}^{BAT\_ch} \leqslant C_{\max,i}^{BAT\_dist}/(\tau \cdot 4) \cdot E_{t,i}^{BAT\_chbin} \quad (32)$$

$$0 \leqslant E_{t,i}^{BAT\_dch} \leqslant C_{\max,i}^{BAT\_dist}/(\tau \cdot 4) \cdot E_{t,i}^{BAT\_dchbin} \quad (33)$$

$$E_{t,i}^{BAT\_dchbin} + E_{t,i}^{BAT\_chbin} \leqslant 1 \quad (34)$$

$$C_{\min}^{BAT\_dist} \leqslant C_t^{BAT\_dist} \leqslant C_{\max}^{BAT\_dist} \quad (35)$$

$$C_t^{BAT\_dist\_total} = \sum_i^K C_{t-1,i}^{BAT\_dist}(1 - \lambda^{BAT\_dist} \cdot \tau) \cdot C_{t-1,i}^{BAT\_dist} + E_{t,i}^{BAT\_dist\_ch} \cdot \eta_{BAT}^{ch} + E_{t,i}^{BAT\_dist\_dch}/\eta_{BAT}^{dch} \quad (36)$$

3.7. Cooling energy sources

For the cooling demand several units are available.

3.7.1. Absorption chiller (ABC)

The absorption chiller is used to convert heat generated by the CCHP unit into cooling energy to meet the cooling demand (Eq. (37)). COP of absorption chiller describes its efficiency. COP^{ABC} used in this paper has a value of 1.1 which is relatively low compared to COP of electric heat pumps for example. But absorption chiller still provides an efficient solution to provide cooling energy since can use the heat produced by CCHP unit that would otherwise not be used for any other purpose.

$$Cool_t^{ABC} = H_t^{CCHP\_ABC} \cdot COP^{ABC} \quad (37)$$

$$0 \leqslant Cool_t^{ABC} \leqslant Cool_{\max}^{ABC} \quad (38)$$

3.7.2. Electric (compression) chiller (EC)

The electric chiller is driven by electrical power to produce cooling energy. (Eq. (39)). COP of electric chiller COP^{EC} is much higher compared to absorption chiller. The value used in this paper is 3.5.

$$Cool_t^{EC} = E_t^{EC} \cdot COP^{EC} \quad (39)$$

$$0 \leqslant Cool_t^{EC} \leqslant Cool_{\max}^{EC} \quad (40)$$

3.7.3. Air condition (AC) units

Households in a distributed manner have installed AC units as a source of cooling energy if that energy is not provided by other source (e.g. EHP). AC units are modelled in a simple way; the input electricity is converted to output cooling with the coefficient of performance COP^{AC} equal to 2.7 (efficiency of conversion of electricity consumption to cooling: output cooling energy/input electrical energy).

$$Cool_{t,i}^{AC} = E_{t,i}^{AC} \cdot COP^{AC} \quad (41)$$

$$0 \leqslant Cool_{t,i}^{AC} \leqslant Cool_{\max,i}^{AC} \quad (42)$$

3.8. Backup diesel generator

Backup diesel generator is modelled in case there is not enough electricity capacity (which can sometimes happen in off-grid

mode) but the startup of this unit is expensive and preferably avoided. The output electrical power of backup diesel generator is limited by its maximum and minimum power (Eq. (43))

$$E_t^{binDIESEL} \cdot E_{\min}^{DIESEL}/\tau \leqslant E_t^{DIESEL} \leqslant E_t^{binDIESEL} \cdot E_{\max}^{DIESEL}/\tau \quad (43)$$

$$H_t^{startupDIESEL} = H_t^{binDIESEL} - H_{t-1}^{binDIESEL} \quad (44)$$

Fuel consumption cost is calculated as input fuel energy divided by energy value of a kilogram of diesel fuel (11.94 kW/kg) multiplied by its price.

$$diesel_t = \frac{1/\eta^{DIESEL} \cdot E_t^{DIESEL}}{11.94} \cdot c^{DIESEL} \quad (45)$$

3.9. Flexible electrical demand and renewable energy sources (RES)

3.9.1. Flexible demand

Percentage of total load that can provide fast response flexible demand is included in MEM model in a simplified way. The percentage p_{flex} is set to be 10% of E_d in all simulation steps. E_t^{flex} is positive for load reduction ("production" effect) and negative for load increase ("consumption effect").

$$-p^{FLEX} \cdot E_t^{d\_total} \leqslant \sum_i^K E_{t,i}^{flex} \leqslant p^{FLEX} \cdot E_t^{d\_total} \quad (46)$$

To ensure that rescheduled demand does not exceed certain limit, the information about the total amount of shiftable loads that are being rescheduled at every time step is preserved in continuous decision variable for flexible demand total capacity (Eqs. (47) and (48)).

$$-C_t^{flex\_max}/\tau \leqslant \sum_i^K C_{t,i}^{flex} \leqslant -C_t^{flex\_max}/\tau \quad (47)$$

$$C_{t,i}^{flex} \leqslant C_{t-1,i}^{flex} - E_{t,i}^{flex} \quad (48)$$

3.9.2. Photovoltaics production (PV) and wind turbine (WT) generation

The production of PV arrays ($E_t^{PV\_real}$) depends on the input data (averaged production of 1 kW installed solar energy). The wind production is modelled similarly, with the yearly input data of a real 1 kW wind power plant (scaled), with the difference that wind can be curtailed:

$$E_t^{wind\_curt} + E_t^{wind\_real} = E_t^{wind} \quad (49)$$

Additionally, developed model has the ability to determine optimal installed capacities of RES, which is the total amount of PV and wind that can be seamlessly integrated into the MEM Therefore, the productions are modified with decision variable representing installed RES capacity:

$$E_t^{wind\_real} = E_t^{wind} \cdot X^{wind} E_t^{PV\_real} = E_t^{PV} \cdot X^{PV} \quad (50)$$

3.10. Demand (heat, cooling and electricity)

3.10.1. Heat demand

Heat demand is modelled with different daily curves for different seasons extracted from data available for United Kingdom [60]. The curves are evenly distributed among all households. In scenario with all units being local household level units, the demand needs to be satisfied according to the following equation:

$$H_{t,i}^d \leqslant H_{t,i}^{CHP} + H_{t,i}^{EHP} + H_{t,i}^{AB} + H_{t,i}^{HS} \quad (51)$$

If MEM configuration with district level units (CCHP or district EHP for example), total demand is met in accordance to the Eq. (52) where houses that do not have access to district system supply themselves locally as shown in (Eq. (51), while district heat balance is maintained.

$$H_t^{d\_tot} \leqslant H_t^{TES} + H_t^{EHP} + H_t^{CHP\_total} + H_t^{EHP\_total} + H_t^{AB\_total} + H_t^{HS} \quad (52)$$

$H_t^{CHP\_total}$ is summation of production of all μCHP units installed in corresponding households. To ensure safe operation of MEM in every simulation step heat waste is allowed:

$$H_t^{waste} \leqslant H_t^{d\_tot} - (H_t^{CCHP} - H_t^{CCHP\_ABC} - H_t^{CCHP\_TES} + H_t^{EHP} + H_t^{CHP\_total} + H_t^{EHP\_total} + H_t^{AB\_total} + H_t^{HS\_total}) \quad (53)$$

3.10.1. Cooling demand

Similar to heating demand, cooling demand is modelled with different demand curves evenly distributed among households. The total cooling demand is met by the production from absorption chiller, electric chiller, household EHP units and household AC units. Effectively, wasted cold is potential excess heat generated by the CCHP plant that could have been used by the absorption chiller or heat storage.

$$Cool_{t,i}^d \leqslant Cool_{t1}^{ABC} + Cool_t^{EC} + Cool_t^{EHP\_total} + Cool_t^{AC\_total} \quad (54)$$

3.10.2. Electricity demand

Electricity demand is represented by different profiles for different seasons based on UK data [60]. All households have access to electrical network and equilibrium between production and consumption has to be constantly maintained (Eq. (55)).

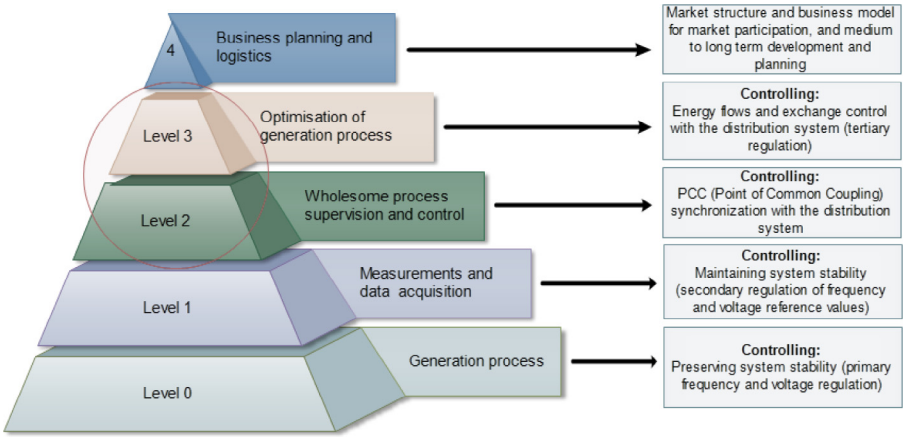

Fig. 5. IEC/ISA 95 standard hierarchy control adjusted for the observed MEM concept.

$$E_i^{d\_tot} + E_t^{\exp} + E_t^{EC} + E_t^{EHP} + E_t^{BAT\_ch} + \sum_i^K E_{t,i}^{EHP} + \sum_i^K E_{t,i}^{BAT\_ch} + \sum_i^K E_{t,i}^{AC} = E_t^{imp} + E_t^{PV\_real} + E_t^{wind\_real} + E_t^{BAT\_dch} + E_t^{diesel} + \sum_i^K E_{t,i}^{flex} + \sum_i^K E_{t,i}^{CHP} + \sum_i^K E_{t,i}^{BAT\_dch} \quad (55)$$

3.11. CO_2 Emissions

Emissions are calculated as in Eq. (43). The emission factors for natural gas, diesel are considered to be constant for energy unit of fuel consumed, while the exchange energy (electricity import/export) equivalent emission are calculated based on average emissions for UK system [61] for electricity generation of each hour.

$$emissions_t = F_t^{ng} \cdot EM^{ng} + F_t^{CCHP} \cdot EM^{CCHP} + F_t^{DIESEL} \cdot EM^{DIESEL} + E_t^{imp} \cdot EM_t + E_t^{\exp} \cdot EM_t \quad (56)$$

F_t^{ng} is the natural gas used by μCHP and auxiliary boiler units, while F_t^{CCHP} is the gas used by the district CCHP unit.

4. Formulation of the receding horizon corrective scheduling model

Trigeneration energy microgrid model described in the previous section is used to test the flexibility benefits of different MEM configurations under receding horizon corrective scheduling control framework.

Microgrid control can be observed as a hierarchical structure (Fig. 5) [62,63]. The lowest level is directly connected with the characteristics of the generator. The second level ensures the stabilization of frequency after the fluctuations. The developed model utilizes a central control system of higher level (Fig. 5– primarily level) with the assumption that the lower level control is efficiently implemented.

The controller for the receding horizon MEM scheduling uses model predictive control scheme (MPC). The basic idea of MPC control is shown in figure below (Fig. 6). The controller based on the reference model results decides on the desired MEM operation. The iterative process dealing with uncertainties runs the optimization with the updated information to MEM central controller/dispatcher. MEM operates according to the market signals, namely energy and balancing prices.

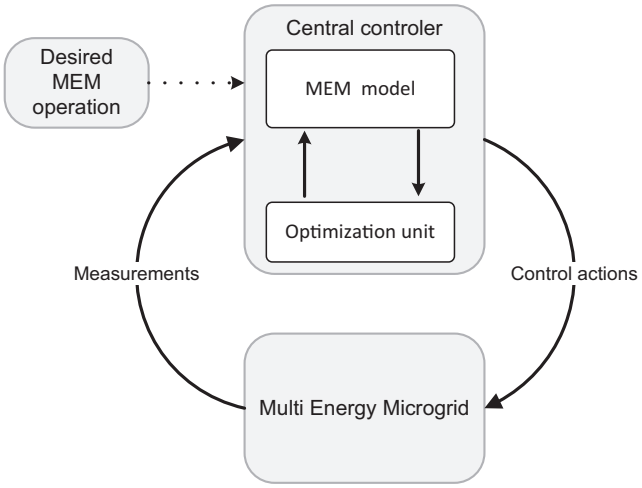

Fig. 6. Model predictive control concept applied to the developed MEM model.

(1) At a certain moment during current day (e.g. 12 h ahead of delivery) MEM sends forecasted energy exchange for the next day at the PCC to the system operator. This exchange is the result of optimization where MEM is considered market price taker.
(2) At the start of the following day (e.g. 00:00 AM) MEM enters the daily cycle where proposed receding horizon MPC algorithm adjusts the operational points of all units in order to follow as closely as possible the plan announced in step 1 by compensating mismatches. In case of deviations due to errors in demand and RES production forecasts, it optimally adjusts operating points of MEM to minimize penalties.

The proposed algorithm is used for correcting initially planned operational points of production units schedules (Corrective) in a manner that always looks ahead till end of the current daily cycle. This means that as the day progresses the corrections are being applied and iteratively planned just for a shortened (Receding) number of future time steps (Horizon) even though the algorithm even in the last time step includes most recent forecasts for the next daily cycle.

Objective function of the proposed MILP model is cast as operational cost minimization. The desired microgrid operation for the reference optimization is driven by the following equation:

$$\text{minimize} COST = \sum_{t=1}^{T_{\max}} \begin{pmatrix} F_t^{ng} \cdot c^{ng} + F_t^{CCHP} \cdot c^{fuel} + F_t^{DIESEL} \cdot c^{diesel} + E_t^{imp} \cdot c_t^{imp} - E_t^{\exp} \cdot c_t^{\exp} \\ +P \cdot E_t^{wind\_cur} + P \cdot H_t^{waste} + H_t^{binCCHP} \cdot c_{const}^{CCHP} + H_t^{startupCCHP} \cdot c_{start}^{CCHP} \\ +E_t^{binDIESEL} \cdot c_{const}^{DIESEL} + E_t^{startupDIESEL} \cdot c_{startup}^{DIESEL} \end{pmatrix} \quad (57)$$

For every simulation step t the control algorithm estimates the system state for the entire operational planning horizon ahead. On the basis of the present state and forecasts for the planning horizon the optimal state is determined. This way both the current state and the future forecast errors are included in the scheduling. More detailed description of the iterative MPC optimization process can be found in [36] or in further literature [64,65] or [66]. For the next simulation step the process is repeated and in each step participation on the balancing (intra-day) market is decided. The operating horizon for the rolling unit commitment model is 24 h which corresponds to the day-ahead scheduling. The most important steps of the optimization algorithm are:

After the initial (reference) run the algorithm uses modified objective function that calculates additional costs due to penalties cause by forecast errors. Index S marks current hour of the day, $E_t^{imp0}, E_t^{\exp 0}$ mark contracted import/export of electricity. Variable $short_t^{imp}$ references to electricity import smaller than contracted due to forecast errors, while $short_t^{\exp}$ is defined for export smaller than contracted. Similarly, $long_t^{imp}$ is defined for electricity import larger than contracted and $long_t^{\exp}$ is defined for positive mismatch in export (export larger than contracted). Factors M^{sell} and M^{buy} are reducing/increasing the market index price to obtain imbalance prices. M^{sell} is smaller than 1 and M^{buy} is larger than 1.

The first line of the objective function (Eq. (58)) models the expected cost for contracted exchange, second segment is mismatch penalty cost. The first two segments represent costs for realized hours of the ongoing day. The third segment represents predicted cost for upcoming hours of the ongoing day (notice that as the RH-MPC progresses closer to the end of the day, values in line 3 are "shifted" into values in line 2, meaning all energy is delivered at the end of the day).

$$
\begin{aligned}
COST = & \sum_{t=1}^{24\cdot\tau+1-S}\begin{bmatrix} F_t^{ng}\cdot c^{ng} + F_t^{CCHP}\cdot c^{fuel} + F_t^{DIESEL}\cdot c^{diesel} + E_t^{imp0}\cdot c_t^{mcp} - E_t^{\exp 0}\cdot c_t^{mcp} + \\ P\cdot E_t^{wind\_cur} + P\cdot H_t^{waste} + H_t^{binCCHP}\cdot c_{const}^{CCHP} + H_t^{startupCCHP}\cdot c_{start}^{CCHP} \\ + E_t^{binDIESEL}\cdot c_{const}^{DIESEL} + E_t^{startupDIESEL}\cdot c_{startup}^{DIESEL} \end{bmatrix} \\
& \left[(-)short_t^{imp}\cdot M^{sell}\cdot c_t^{mcp} + long_t^{imp}\cdot M^{buy}\cdot c_t^{mcp} + short_t^{\exp}\cdot M^{buy}\cdot c_t^{mcp} - long_t^{\exp}\cdot M^{sell}\cdot c_t^{mcp}\right] + \\
& + \sum_{t=24\cdot\tau+1-S}^{24\cdot\tau}\begin{bmatrix} F_t^{ng}\cdot c^{ng} + F_t^{CCHP}\cdot c^{fuel} + F_t^{DIESEL}\cdot c^{diesel} + E_t^{imp}\cdot c_t^{imp} - E_t^{\exp}\cdot c_t^{\exp} \\ + P\cdot E_t^{wind\_cur} + P\cdot H_t^{waste} + H_t^{binCCHP}\cdot c_{const}^{CCHP} + H_t^{startupCCHP}\cdot c_{start}^{CCHP} \\ + E_t^{binDIESEL}\cdot c_{const}^{DIESEL} + E_t^{startupDIESEL}\cdot c_{startup}^{DIESEL} \end{bmatrix}
\end{aligned}
\tag{58}
$$

All modelled element parameters are listed and explained in Table 2. Elements in different simulations have different installed capacities (e.g. TES capacity, household type, shares or households, battery storage capacity) due to different MEM configurations. For

Table 2
Parameter values.

Parameter	Value [Unit]
Simulation time $T_{\max}$	24–8760 [h]
Simulation time step duration τ	2 (30 min) [hour segments]
Number of households in district MEM K	e.g. 300
Penalty factor for unused energy P	e.g. 300
Natural gas price c^{ng}	0.025 [€/kW h]
CCHP unit fuel gas price c^{cchp}	0.024 [€/kW h]
Diesel price c^{diesel}	0.037 [€/kW h]
Flexible demand share p^{flex}	10 [%]
Maximum flex demand capacity $C_{\max}^{flex}$	50 [kW h]
Electric efficiency of μCHP unit $\eta_i^{chp\_e}$	24 [%]
Thermal efficiency of μCHP unit $\eta_i^{chp\_h}$	54 [%]
Electric efficiency of district CCHP unit $\eta_i^{cchp\_e}$	32 [%]
Thermal efficiency of district μCHP unit $\eta_i^{cchp\_h}$	55 [%]
Maximum fuel intake power of district CCHP unit $H_{\max}^{CCHP}$	1000 [kW h_t]
Maximum thermal output of district CCHP unit $H_{\max}^{CCHP}$	≈550 [kW h_t]
Maximum thermal output of μCHP unit $H_{\max,i}^{CHP}$	8 [kW h_t]
Maximum thermal/cooling output of EHP unit $H_{\max,i}^{EHP}$	10 [kW h_t]
Maximum power output of EHP unit $H_{\max}^{EHP}$	300 [kW h_t]
Share of households with CHP based heating	40 [%]
Share of households with EHP based heating	30 [%]
Share of households with only boiler based heating	30 [%]
Mean coefficient of performance for household EHP units COP_t	3.5 summer 3.0 inter (sprint, autumn) 2.5 winter
Coefficient of performance for district EHP unit COP	6.0 summer 5.0 inter (sprint, autumn) 4.5 winter
Maximum thermal output of a boiler unit $H_{\max,i}^{AB}$	10 [kW h_t]
Auxiliary boiler efficiency η^{AB}	85 [%]
District thermal energy storage maximum capacity $C_{\max}^{TES}$	2000 [kW h_t]
Household heat storage maximum capacity $C_{\max,i}^{hs}$	6 [kW h_t]
Heat storage efficiency η_{hs}	98 [%]
Household battery storage maximum capacity $C_{\max,i}^{bat}$	4 [kW h_e]
Central battery storage maximum capacity $C_{\max}^{bat}$	50 [kW h_e]
Maximum power output of a backup diesel unit $H_{\max,i}^{AB}$	50 [kW h_t]
Backup diesel efficiency η^{AB}	33 [%]
Coefficient of performance of electric chiller COP^{EC}	3.5 [–]
Coefficient of performance of absorption chiller COP^{AC}	1.2 [–]
Coefficient of performance of household AC unit COP_i^{AC}	2.7 [–]
Electric chiller unit maximum cooling power $Cool_{\max}^{EC}$	50 [kW h]
Household AC unit maximum cooling power $Cool_{\max,i}^{AC}$	5 [kW h]
Installed wind capacity X^{wind}	50 [kW]
Installed PV capacity X^{wind}	200 [kW]

Table 3
Dependence of the MEM capability to integrate RES on the μCHP technology used.

μCHP technology	Efficiency [%]		Optimal PV installed capacity [kW]		Optimal WIND installed capacity [kW]		Total emissions [tons]		Percent of demand met from RES [%]	
	Elec.	Therm.	No bat.	Bat.	No bat.	Bat.	No bat.	Bat.	No bat.	Bat.
Fuel cell	30	55	92	102	71	68	840	834	37.93	38.77
Stirling engine	20	77	70	89	184	180	799	795	61.98	62.24
Comb. engine	26	64	70	81	108	101	817	810	45.78	46.44
Steam engine	24	70	68	79	135	130	808	801	51.81	52.30
μ gas turbine	24	55	65	88	97	91	863	856	43.21	43.63

the sake of simplicity, the paper does not focus on optimal sizing of the units (which was performed), but rather focuses on providing insight into differences between scheduled and realized operational points and how their plan changes as the time progresses. Furthermore, it captures the impact of efficiency modelling approximations on different operational horizons.

The simulation model was developed using FICO Xpress 7.9 [67] and MATLAB 2015 [68] and run on laptop with Intel i5 @2.3 GHz processor with 8 GB RAM with gap tolerance of 0.05%.

5. Annual operation results

5.1. Flexibility analysis of different μCHP technologies

Developed multi-energy microgrid operation was simulated for 17,520 half-hourly time steps. The available flexibility of the microgrid is measured through waste of energy (heat and curtailed wind expressed in kW h) indicator. In off-grid mode, MEM needs to have enough capacity and flexibility to satisfy the demand in all simulation steps. In on grid mode mismatch in kW h between scheduled (contractual) and realized export/import values of electricity serves as a flexibility indicator.

The initial analyses focus on impact of battery storage and different technologies of distributed generation, characterized by different efficiencies. The results clearly demonstrate specific elements have higher impact in terms of provision of flexibility.

The results from a set of simulations for different μCHP technologies [69] are shown in Table 3. The assumed configuration of MEM is Type 1 (Table 1 – distributed). Total share of μCHP units in households is set to 40%, share of EHP units 30%, while the rest of the households are equipped with boilers as a heating source. Off-grid operation mode was analyzed. It can be seen that the capability of a multi-energy microgrid to integrate RES is highly dependent on the μCHP unit technology since it represents the most significant heat source in the distributed configuration.

Observing the amount of wasted energy, as an operation efficiency indicator, for all the μCHP technologies, the addition of battery storage in all cases reduces unused energy (Fig. 7). Additionally, it is interesting to observe that technologies with more efficient heat production have higher percentage of curtailed wind. Heat and electricity production are correlated, meaning that in heat following mode excess electricity will be produced by μCHP.

5.2. Flexibility aspects of different MEM configurations

Different MEM configurations (Table 1) manifest different operational capabilities (Fig. 8). Highest operational costs are obtained for Type 1 (distributed/household) since smaller units with lower efficiency are used, while the best "performance" is seen for Type 3 and Type 4 where a combination of distributed and centralized units are participating in MEM portfolio.

Since in MEM parallel operation with the system waste of energy is close to zero, more interesting conclusions can be drawn for the off-grid mode. Interestingly, now the lowest waste is achieved for Type 1 configuration. The reason for that is partially that μCHP units do not have ramping or minimum stable operation constraints (as mentioned in previous Section 3.2). However, a general conclusion is that Type 3 (combination of district heating system and household EHP units) has the best trade-off in terms of amount of wasted energy and total costs.

Interesting aspect of annual operational results is seen when adding another energy vector – cooling. The results presented in Fig. 9 show the comparison in energy mix for the case when all cooling demand is met by electrically driven elements (e.g. household AC and EHP) and when separate energy vector of cooling demand is regarded through heat use in absorption chiller. The

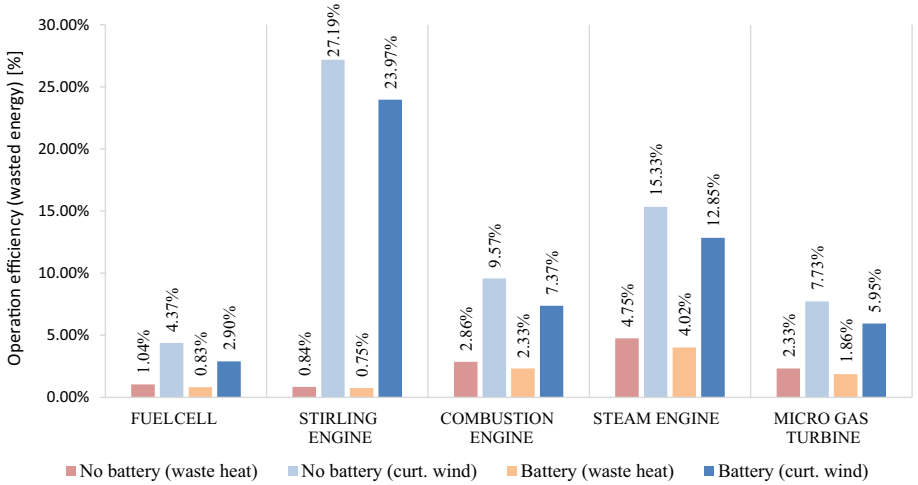

Fig. 7. Unused energy for multi-energy microgrid with different μCHP technologies (in percent to total heat used || total wind energy production).

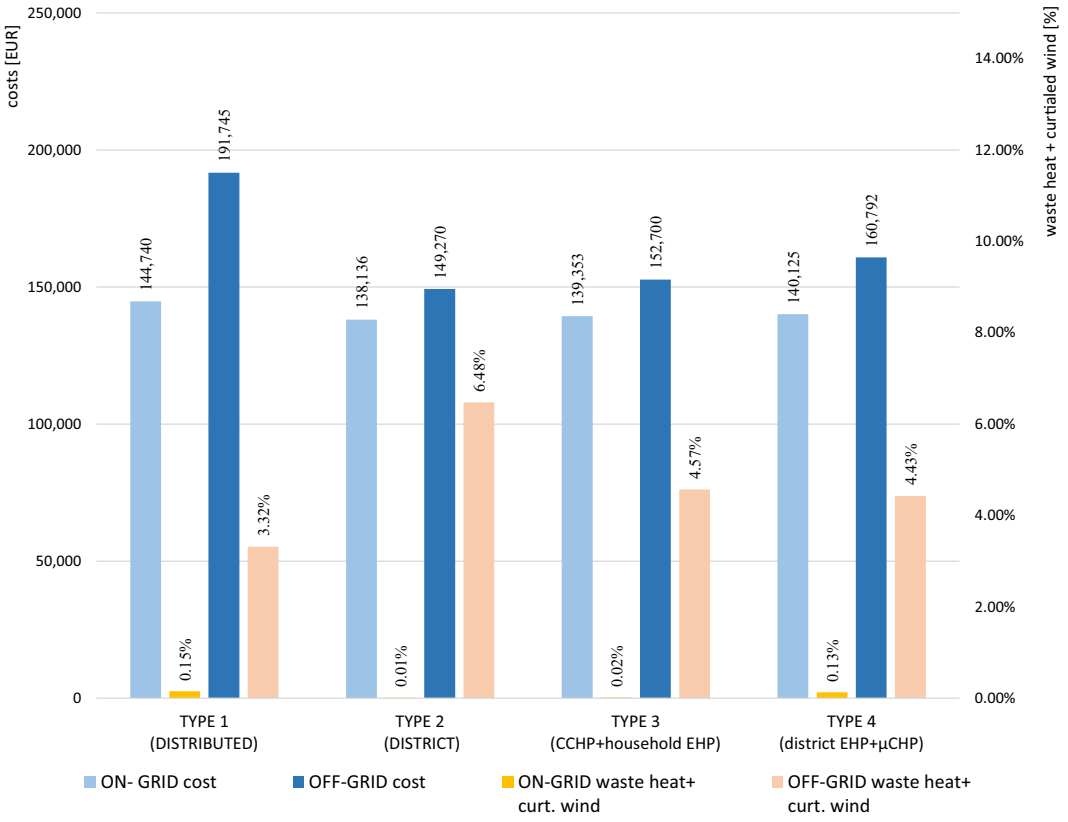

Fig. 8. Operational indicators for different MEM configurations.

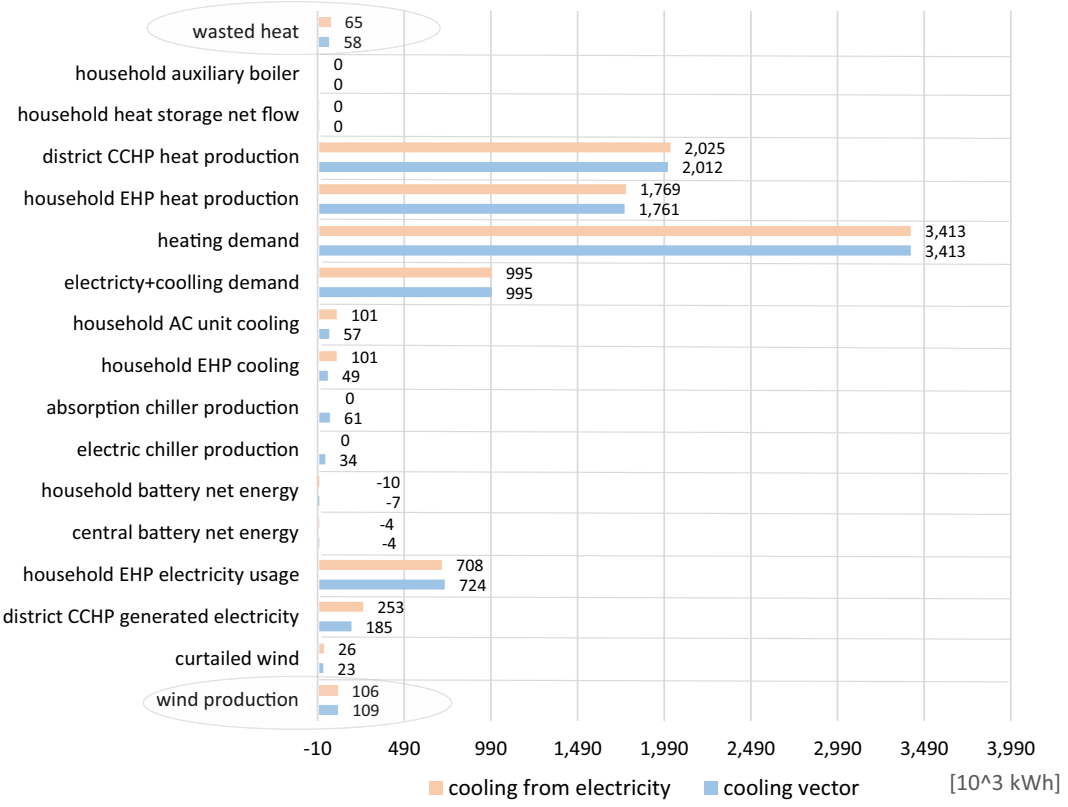

Fig. 9. Comparison of MEM operation for different cooling modes (cooling from electricity VS separate cooling vector).

assumed operation is off-grid. It can be seen that with the separate cooling vector the curtailment of wind is reduced from 24.15% to 20.90% (which equals to 2838 kW h) and waste of heat is reduced from 1.90% to 1.70% (which equals to 6761 kW h). Additionally, operating costs are reduced approximately 21% (from 193,700 EUR to 153,000 EUR), clearly showing flexibility benefits achieved by coupling multiple energy vectors.

Annual operation analyses of MEM with different efficiency modelling approaches (constant value efficiency versus load dependent efficiency) show that the total costs difference for off grid simulation is maximum for Type 3 and is 5.87%. What is more important to observe is the daily behavior of the CCHP operation and the differences that stem from two efficiency modes. The following Section (-section VI) explains the main principals of developed RH-MPC corrective control algorithm and shows the importance of deploying such algorithm during the daily operation cycle.

6. Daily operational analyses

Daily operational analyses are based on receding horizon with model predictive control (RH-MPC) where MEM is operating parallel to the rest of the power system. In between two successive days MEM is trying to follow the scheduled (contracted) exchanges based on the optimal production plan for 24 h-ahead period. The initial scheduled plan (marked with time step '0') is susceptible to changes due to stochastic element inherent to predictions of demand fluctuations and RES production (included through corresponding probability density functions). In deterministic environment, scheduled and announced operational plan would be fulfilled in every segment. However, realistic, stochastic environment implies that MEM needs to flexible enough to follow scheduled exchanges with the upstream system, in order to avoid

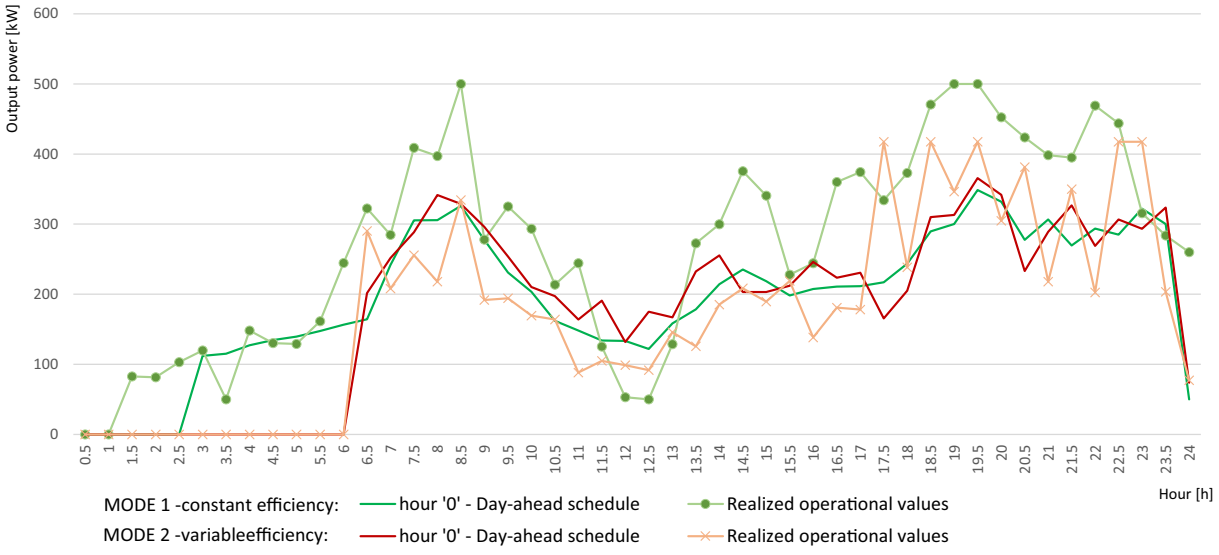

Fig. 10. Scheduled vs. realized values of CCHP plant heat production for a winter day with non-forecasted temperature drop that caused increased heat demand (+10% heating energy used throughout the whole day).

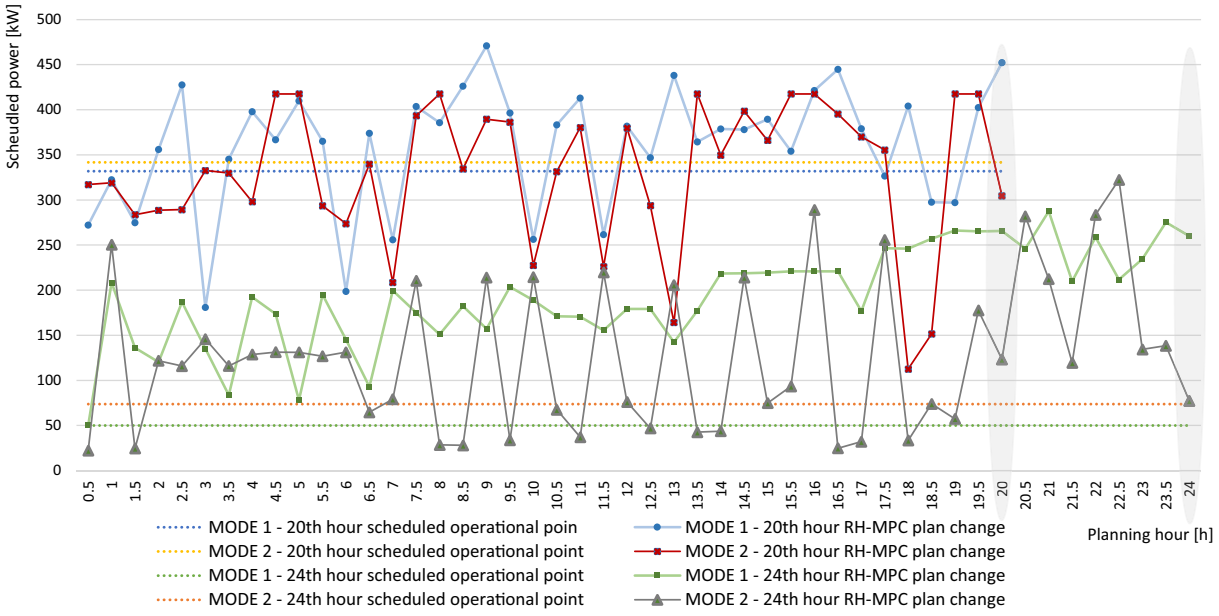

Fig. 11. RH-MPC planned values for last hour of the receding horizon (48th time step) each time step throughout the current day-ahead cycle.

imbalance costs and act in a most beneficial way for the rest of the power system.

Developed corrective control strategy, based on model predictive control, calculates for each time step the optimal MEM operation for the entire look-ahead horizon and applies corrective measures only from current time step till the end of the current planning cycle (24 h cycle of the day-ahead market). The algorithm, as mentioned before, takes into account the intra-day imbalance market [70].

The difference in planned and realized values of operational points of CCHP, also for different efficiency modelling, are depicted in Fig. 10 for a winter day simulation. It shows the difference between constant efficiency and variable efficiency mode. For brevity and easier understanding of figures, modelling efficiencies as approximated constant value is referred to as MODE 1, while load depending value of efficiency is referred to as MODE 2.

Already in the initial day-ahead schedule (*hour '0'*) of CCHP operating points, the differences are noticeable (green and red line on Fig. 10). Although schedules for both modes of efficiencies are of similar shaped, different operating points in early periods of the day indicate approximations in modelling are highly relevant and can result in incorrect assumptions.

Furthermore, comparing final operational values (resulting from intra-day adjustments by RH-MPC) the difference between electricity exchanged with the upstream system and MEM is noticeable (e.g. during time steps 8–11) suggesting approximations do not provide accurate results relevant to short term operation (green line and orange line with marker on Fig. 10). Fig. 11 shows two different sets of values: first set (dotted lines) shows the planned value for CCHP output made at the start of the day-ahead cycle (again, for efficiency approximation and loading dependent efficiency). Second (line with markers) shows how the planned operational point for a specific hour changes dynamically in each time step. More precisely, planned operational point for a specific hour (e.g. 20th hour) in each planning step is shown on the graph as *"RH-MPC plan change"*. The final operational value (moment when the plan of the last planning horizon is realized) is shaded (Fig. 11). As it can be seen the difference between two efficiency modes is visible both thorough the rolling of the RH-MPC process and through difference in finally realized output

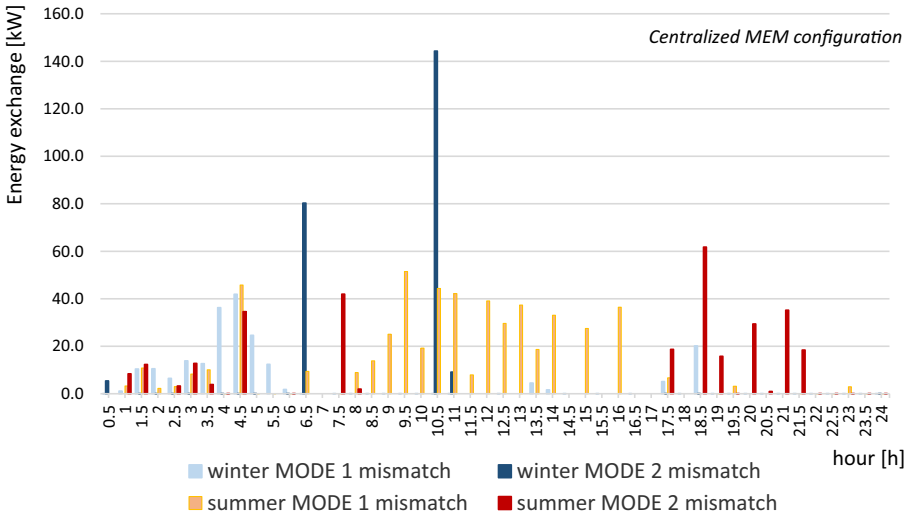

Fig. 12. Mismatch between scheduled (contractual) and realized electricity exchanges for both efficiency modelling approaches in centralized MEM configuration.

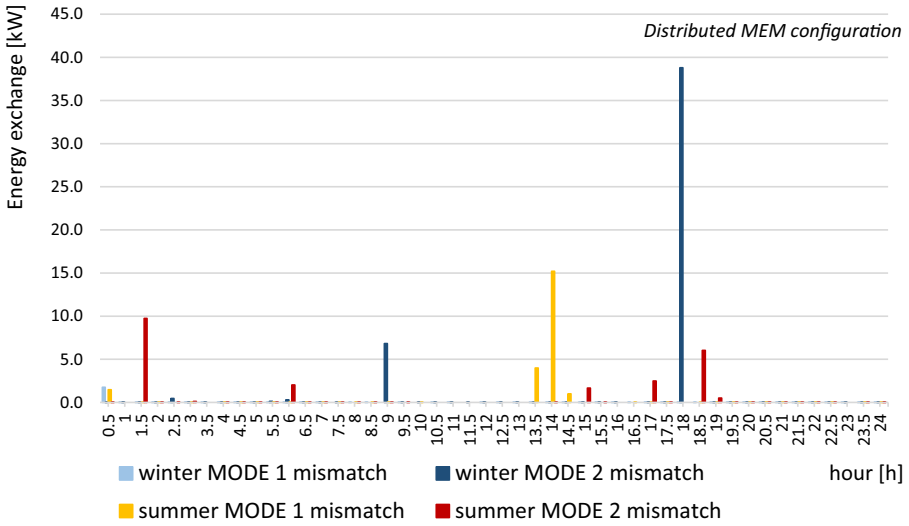

Fig. 13. Mismatch between scheduled (contractual) and realized electricity exchanges for both efficiency modelling approaches in distributed MEM configuration.

power. Mode 2 manifests in steeper changes in plan since the simulation tries to run the production units close to minimum generation or close to highest possible generation in that particular moment.

Flexibility indicator in on-grid operation is represented through a mismatch between the contractual (scheduled) and realized values of import/export electricity. For different MEM configurations, namely distributed and centralized, the mismatch values are shown in Figs. 12 and 13. During summer periods available flexibility is lower due to lower heat demand visible as higher mismatch values. Absolute values of exchange mismatches compared to the total contractual exchange can be noted from Fig. 14.

When comparing the mismatch error for different efficiency modes it can be concluded that on average MODE 1 yields better flexibility indicators (from 10 simulated winter and summer days). Additionally, when observing the precise moment mismatches occur the difference is noticeable. The total exchange volume is on average larger for efficiency MODE 1 (constant efficiency) as can be seen from Fig. 14.

As a final conclusion it should be noted that approximations in modelling lead to over, or under, estimating available flexibility and results in different operating points of MEM units. These errors are highly relevant in on-grid operation as they give incorrect information to the system operator.

6.1. Simulation duration

Total duration of the simulation is important when in a daily cycle the optimization at each step (e.g. every 15 or 30 min) needs to be finished. The total duration of the RH-MPC corrective algorithm depends on the efficiency mode used (Table 4). In daily operation simulation each step simulation needs to be finished in approximately 5 s, which sums up to approximately 10 min total if 15-min time steps are used (96 × 5 s + data cycling). For majority of the days the simulation is finished within the given time frame but there are exceptions for the efficiency mode 2 when single step simulation lasts even 30 s (only for a few selected summer days). This means that even though the importance of having more precise efficiency modelling is significant both in terms of cost and operational points in daily operation, using constant efficiency mode approximations guarantees every simulation will be short enough even on an average personal computer. It worth noting that values presented in Table 4 represent maximum duration of a single step and only for the longest possible horizon of the entire day. Average duration is shorter and the whole iterative process at every time step lasts between 200 and 500 s depending on the configuration and simulation setup. In practice, the look-ahead horizon of 8 h (so reducing it to 16 of 32 simulation time steps) might be enough, ensuring satisfactory simulation duration in all possible cases.

6.2. Daily operational analyses discussion

To wrap up the results sections the following conclusions can be made regarding the different aspects of conducted simulations:

(i) Multi-energy microgrid configuration:
- Microgrids perform differently depending on their configurations and aggregation. The results clearly show that although centralized unit MEM has lower operational

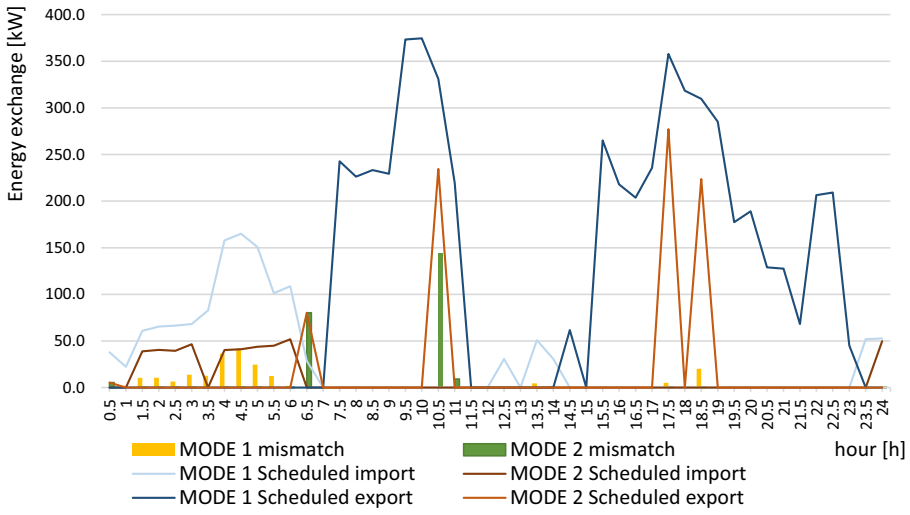

Fig. 14. Contractual exchanges for a winter day simulation for different efficiency modes.

Table 4
Simulation duration for on-grid mode (30 min time step).

	Total simulation duration [min]		Single iterative step maximum simulation duration [s]		Single iterative step average simulation duration [s]	
	MODE 1	MODE 2	MODE 1	MODE 2	MODE 1	MODE 2
Annual operation – Type 1 (distributed)	141.16	373.50	–	–	–	–
Annual operation – Type 2 (centralized)	130.25	358.78	–	–	–	–
Annual operation – Type 3 (CCHP + household EHP)	129.55	360.12	–	–	–	–
Annual operation – Type 4 (district EHP + μCHP)	122.92	300.19	–	–	–	–
RH-MPC daily operation – Type 1 (distributed)	7.68	22.41	4.91	29.42	1.43	4.82
RH-MPC daily operation – Type 2 (centralized)	6.85	19.26	2.84	26.33	0.75	4.22

costs, fully distributed MEM configuration (all household units) is capable of integrating more local RES production.
- Adding energy vectors, such as cooling, to MEM configuration results in higher flexibility manifested as lower operational costs and lower wasted energy.

(ii) Efficiency mode used:
- Efficiency of production units, in particular CHP, has large impact on overall MEM operation (shown in Table 3 results).
- Differences in annual operational costs between constant efficiency mode (mode 1) and variable efficiency depending on the loading (mode 2) are in range of 2–5%. This shows approximations do not have significant effect in long term operational analyses.
- Difference in daily operational costs between constant efficiency mode (mode 1) and variable efficiency depending on the loading (mode 2) are significant and manifest is different unit operational points as well as larger mismatches for in exchange with the system. This indicates that approximations have high impact on short term schedules.;

7. Conclusion and future work

The paper presents a comprehensive multi-energy microgrid model that incorporates flows of different energy vectors: heating, cooling, electricity and fossil fuel. The developed model is linear (MILP) which guarantees optimality of the results. The model is used to track the operation of different MEM configurations through defined flexibility indicators for both off-grid operation (wasted heat and curtailed wind) and on-grid operation (waste of energy and mismatch from contractual electricity import/export). On top of this, impact of efficiency modelling (constant efficiency vs. variable efficiency depending on loading) is analyzed. The results show that there is a significant operational difference both in cost and flexibility indicators when comparing different MEM configurations composed of different production units. Furthermore, efficiency modelling aspect impacts both the process of developed receding horizon corrective control and final operational points of production units.To summarize, following findings can be highlighted:

(a) Regarding the MEM configuration, combination of centralized and distributed configurations gives the best performance.
(b) Regarding the coupling of energy vectors, adding additional separate energy vectors (e.g. cooling) increases flexibility by reducing total cost, wasted energy and curtailed RES.
(c) Regarding the efficiency modelling, total costs on an annual basis are very similar regardless of the efficiency mode used (constant efficiency and variable efficiency).
(d) Regarding the daily corrective RH-MPC algorithm, on a daily level the results for different efficiency mode are significantly different due to more frequent unit cycling in variable efficiency modelling scenarios.

Further investigation will be headed into the direction of defining flexibility maps for the production units that would in every moment give information how much flexibility, how long and at what cost can be provided. In addition to that, further details regarding the interaction between the energy vectors will be studied as well as the addition of EV vehicles and their inherent stochastic behavior. Furthermore, operational limits of district energy infrastructure will be included in a more detailed fashion. Horizon lengths impact will also be considered to reduce the overall computational time.

Acknowledgment

The work of the authors is a part of the project IRES-8 Instigation of Research and Innovation Partnership on Renewable Energy, Energy Efficiency and Sustainable, Energy Solutions for Cities funded by European Union and FENISG- Flexible Energy Nodes in Low Carbon Smart Grid funded by Croatian Science Foundation under project grant No. 7766.

References

[1] Pollit MG. The future of electricity (and gas) regulation in a low-carbon policy world. Energy J 2008;29:63–94.
[2] Siano P. Assessing the impact of incentive regulation for innovation on RES integration. IEEE Trans Power Syst 2014;29:2499–508.
[3] Baringo L, Conejo AJ. Wind power investment within a market environment. Appl Energy 2011;88(9):3239–47.
[4] Manfren M, Caputo P, Costa G. Paradigm shift in urban energy systems through distributed generation: methods and models. Appl Energy 2011;88 (4):1032–48.
[5] Meibom P, Hilger KB, Madsen H, Vinther D. Energy comes together. IEEE Power Energy Mag 2013;11(5):46–55.
[6] Banovac E, Stojkov M, Kozak D. Designing a global energy policy model. Energy 2017;170:2–11.
[7] European Commission. Communication from the Commission: clean energy for all Europeans; 2016.
[8] Pavić I, Capuder T, Kuzle I. Low carbon technologies as providers of operational flexibility in future power systems. Appl Energy 2016;168:724–38.
[9] Olivares E, Mehrizi-Sani A, Etemadi AH, Canizares CA, Iravani R, Kazerani M, et al. Trends in microgrid control. IEEE Trans Smart Grid 2014;5:1905–19.
[10] Hakimi M, Moghaddas-Tafreshi SM. Optimal planning of a smart microgrid including demand response and intermittent renewable energy resources. IEEE Trans Smart Grid 2014;5:2889–900.
[11] Dietrich K, Latorre JM, Olmos L, Ramos A. Demand response in an isolated system with high wind integration. IEEE Trans Power Syst 2012;27:20–9.
[12] Lannoye E, Flynn D, O'Malley M. Evaluation of power system flexibility. IEEE Trans Power Syst 2012;27:922–31.
[13] Group of authors. Flexibility in 21st Century Power Systems. National Renewable Energy Laboratory; 2014.
[14] Troy N, Denny E, O'Malley M. Base-loadcycling on a system with significant wind penetration. IEEE Trans Power Syst 2010;25:1088–97.
[15] Morvaj B, Evins R, Carmeliet J. Decarbonizing the electricity grid: The impact on urban energy systems, distribution grids and district heating potential. Appl Energy 2017;191:125–40.
[16] Morvaj B, Evins R, Carmeliet J. Optimization framework for distributed energy systems with integrated electrical grid constraints. Appl Energy 2016;171:296–313.
[17] Knezovic K, Martinenas S, Andersen PB, Zecchino A, Marinelli M. Enhancing the role of electric vehicles in the power grid: field validation of multiple ancillary services. IEEE Trans Transport Electrification 2016; 99.
[18] Hatziargyriou N, Asano H, Iravani R, Marnay C. Microgrids. IEEE Power Energy Mag; 2007.
[19] Pandzic H, Kuzle I, Capuder T. Virtual power plant mid-term dispatch optimization. Appl Energy 2011;101:134–41.
[20] Mashayekh S, Stadler M, Cardoso G, Heleno M. A mixed integer linear programming approach for optimal DER portfolio, sizing, and placement in multi-energy microgrids. Appl Energy 2017;187:154–68.
[21] Hanna R, Ghonima M, Kleissl J, Tynan G, Victor DG. Evaluating business models for microgrids: Interactions of technology and policy. Energy Policy 2017;103:47–61.
[22] Dvorkin Y, Fernandez-Blanco R, Kirschen DS, Pandzic H, Watson J-P, Silva-Monroy CA. Ensuring profitability of energy storage. IEEE Trans. Power Syst. 2016; PP(99): p. 1–1.
[23] Mancarella P. MES (multi-energy systems): an overview of concepts and evaluation models. Energy 2014;65:1–17.
[24] Good N, Karangelos E, Navarro-Espinosa A, Mancarella P. Optimization under uncertainty of thermal storage-based flexible demand response with quantification of residential users' discomfort. IEEE Trans Smart Grid 2015;6 (5):2333–42.
[25] Majzoobi A, Khodaei A. Application of microgrids in providing ancillary services to the utility grid. Energy; 2017.
[26] Saint-Pierre A, Mancarella P. Active distribution system management: a dual-horizon scheduling framework for DSO/TSO interface under uncertainty. IEEE Trans. Smart Grid 2016; p. 1–12.
[27] Capuder T, Mancarella P. Assessing the benefits of coordinated operation of aggregated distributed multi-energy generation. In: Power system computation conference (PSCC) 2016; 2016. p. 1–7.
[28] Cui H, Li F, Hu Qinran, Bai L, Fang X. Day-ahead coordinated operation of utility-scale electricity and natural gas networks considering demand response based virtual power plants. Appl Energy 2016;176:183–95.
[29] Ghahgharaee Zamani A, Zakariazadeh A, Jadid S. Day-ahead resource scheduling of a renewable energy based virtual power plant. Appl Energy 2016;169:324–40.

[30] Rahimiyan M, Baringo L. Strategic bidding for a virtual power plant in the day-ahead and real-time markets: a price-taker robust optimization approach. IEEE Trans Power Syst 2016;31(4):2676–87.
[31] Zhang N, Kang C, Xia Q, Huang Y. A convex model of risk-based unit commitment for day-ahead market clearing cosidering wind power uncertainty. IEEE Trans Power Syst 2014; 30(3): p. 1582–1592.
[32] Baringo A, Baringo L. A stochastic adaptive robust optimization approach for the offering strategy of a virtual power plant. IEEE Trans Power Syst 2016; 8950(c): p. 1–1.
[33] Chicco G, Mancarella P. Matrix modelling of small-scale trigeneration systems and application to operational optimization. Energy Mar. 2009;34(3):261–73.
[34] Capuder T, Mancarella P. Techno-economic and environmental modelling and optimization of flexible distributed multi-generation options. Energy 2014.
[35] Wang H, Mancarella P. Towards sustainable urban energy systems: high resolution modelling of electricity and heat demand profiles. In: Powercon, 2016, pp. 1–6
[36] Holjevac N, Capuder T, Kuzle I. Adaptive control for evaluation of flexiblity benefits in microgrid system. Energy 2015;52:487–504.
[37] Mancarella P, Chicco G. Demand response from energy shifting in distributed multi-generation. IEEE Trans Smart Grid 2013;4(4):1928–38.
[38] Holjevac N, Capuder T, Kuzle I. Defining key parameters of economic and environmentally efficient residential microgrid operation. Energy Procedia 2017;105C:999–1008.
[39] Schütz T, Harb H, Streblow R, Müller D. Comparison of models for thermal energy storage units and heat pumps in mixed integer linear programming. In: The 28th international conference on Efficiency, Cost, Optimization, Simulation and Environmental Impact of Energy Systems, ECOS 2015, Pau, France; 2015.
[40] Zhang L, Capuder T, Mancarella P. Unified unit commitment formulation and fast multi-service LP model for flexibility evaluation in sustainable power systems. IEEE Trans Sustain Energy 2016;7(2):658–71.
[41] Henwood MI, van Ooijen M. An algorithm for combined heat and power economic dispatch. IEEE Trans Power Syst 1996;11:1778–84.
[42] Verda V, Colella F. Primary energy savings through thermal storage in district heating networks. Energy 2011;36:4278–86.
[43] Papaefthymiou G, Hasche B, Nabe C. Potential of heat pumps for demand side management and wind power integration in the German electricity market. IEEE Trans Sustain Energy 2012;3:636–42.
[44] Capstone C1000 Series Microturbine System Technical Reference. Capstone Turbine Corporation, Chatsworth, CA, USA, Tech. Rep. 410066, Rev B; 2011.
[45] Fang F, Wang Q, Shi Y. A novel optimal operational strategy fort he CCHP system based on two operating modes. IEEE Trans Power Syst May 2012;27 (2):1032–41.
[46] Capstone C30 Microturbine Technical Reference. Capstone Turbine Corporation, Chatsworth, CA, USA, Tech. Rep. 410066, Rev H; 2006.
[47] Capstone C200 Microturbine Technical Reference. Capstone Turbine Corporation, Chatsworth, CA, USA, Tech. Rep. 410066, Rev C; 2009.
[48] Krishna CR. Performance of the Capstone C30 Microturbine on Biodisel Blends. Upton NY, USA: Brookhaven National Laboratory; 2007.
[49] Xiao X, Zheng G, Kan W, Chen X, Wang B, Wang T. Study on the structure and control system of Capstone C200 Microturbine. Gas Turbine Technol Dec 2010;23(4):18–21.
[50] Acadia Heat Pump Technical Brouchure, Hallowell Iternational, EnergyIdeas Claringhouse, PTR #19; December 2007.
[51] Data Sheet LA 12TU heat pump. Glen Dimplex Germany; November 2016.
[52] Nagota T, Shimoda Y, Mizuno M. Verification of the energy-saving effect of the district heating and cooling system—Simulation of an electric-driven heat pump system. Energy Build 2008;40:732–41.
[53] Chua KJ, Chou SK, Yang WM. Advances in heat pump sysmtes: A review. Appl Energy 2010;87:3611–24.
[54] Good N, Navarro-Espinosa A, Karangelos E, Mancarella P. Participation of electric heat pump resources in electricity markets under uncertainty. In: Proceedings of 10th Int. Conference on the European Energy Market; 2013.
[55] Almassalkhi MR, Towle A. Enabling city-scale multi-energy optimal dispatch with energy hubs. Power Systems Computation Conference (PSCC); 2016.
[56] Labidi M, Eynard J, Faugeroux O, Grieu S. A new strategy based on power demand forecasting to the management of multi-energy district boilers equipped with hot water tanks. Appl Therm Eng 2017;113:1366–80.
[57] Dincer I. Thermal energy storage systems as a key technology in energy conservation. Int J Energy Res 2002;26:567–88.
[58] Chen X, Kang C, O'Malley M, Xia Q. Increasing the flexibility of combined heat and power for wind power integration in China: modeling and implications. IEEE Trans Power Syst 2015;30(4):1848–57.
[59] Li G, Zhang R, Jiang T, Chen H, Bai L, Cui H, Li X. Optimal dispatch strategy for integrated energy systems with CCHP and wind power. Appl Energy 2017;192:408–19.
[60] Demand profile generators. University of Strathclyde; December 2016. online: http://www.strath.ac.uk.
[61] Capuder T, Mancarella P. Techno-economic and environmental modelling and optimization of flexible distributed multi-generation options. Energy 2014;71:516–33.
[62] Guerrero JC, Vasquez J, Vicuña LG, Castilla M. Hierarchical control of droop-controlled AC and DC microgrids—a general approach toward standardization. IEEE Trans Ind Electron 2011;58:158–72.
[63] Ambrosio R, Widergren SE. A framework for addressing interoperability issues. IEEE PES General Meeting; 2007. p. 1–5.
[64] Marinelli M, Sossan F, Costanzo GT, Bindner H. Testing of a predictive control strategy for balancing renewable sources in a microgrid. IEEE Trans Sustain Energy 2014;5:1426–33.
[65] Larsen G, van Foreest N, Scherpen J. Distributed MPC applied to a network of households with micro-CHP and heat storage. IEEE Trans Smart Grid 2014;5:2106–14.
[66] Parisio A, Rikos E, Tzamalis G, Glielmo L-. Use of model predictive control for experimental microgrid optimization. Appl Energy 2014;1(15):37–46.
[67] FICO Xpress, online Dec. 2016: www.fico.com
[68] MathWorks MATLAB, online Dec. 2016: www.mathworks.com
[69] Jablko R, Saniter C, Hantisch R, Holler S. Technical and economical comparison of micro CHP systems. In: 2005 International Conference on Future Power Systems. Amsterdam, Netherlands; 2005. p. 1-6.
[70] Elexon Imbalance Pricing Guidance – A guide to electricity imbalance pricing in Great Britain, version 11.0, Oct. 2016.